

1 **Controls on spatial and temporal variability of streamflow** 2 **and hydrochemistry in a glacierized catchment**

3 **Running title: Controls on streamflow and hydrochemistry in a glacierized catchment**

4 Michael Engel¹, Daniele Penna², Giacomo Bertoldi³, Gianluca Vignoli⁴, Werner Tirler⁵, and
5 Francesco Comiti¹

6 ¹Faculty of Science and Technology, Free University of Bozen-Bolzano, Piazza Università 5,
7 39100 Bozen-Bolzano, Italy

8 ²Department of Agricultural, Food and Forestry Systems, Via S. Bonaventura, 13, University
9 of Florence, 50145 Florence, Italy

10 ³Institute for Alpine Environment, Eurac Research, Viale Druso 1, 39100 Bozen-Bolzano,
11 Italy

12 ⁴CISMA S.r.l., Via Volta 13/A, 39100 Bozen-Bolzano, Italy

13 ⁵Eco-Research S.r.l., Via Negrelli 13, 39100 Bozen-Bolzano, Italy

14

15 *Correspondence to:* Michael Engel (Michael.Engel@unibz.it)

16

17 **Abstract**

18 Understanding the hydrological and hydrochemical functioning of glacierized catchments
19 requires the knowledge of the different controlling factors and their mutual interplay. For this
20 purpose, the present study was carried out in two sub-catchments of the glacierized Sulden
21 River catchment (130 km², Eastern Italian Alps) in 2014 and 2015, characterized by similar
22 size but contrasting geological setting. Samples were taken at different space and time scales
23 for analysis of stable isotopes in water, electrical conductivity, major, minor and trace
24 elements.

25 At the monthly sampling scale, complex spatial and temporal dynamics for different spatial
26 scales (0.05 – 130 km²) were found, such as contrasting electrical conductivity gradients in
27 both sub-catchments were found. At the daily scale, for the entire Sulden catchment the
28 relationship between discharge and electrical conductivity showed a monthly hysteretic
29 pattern. Hydrometric and geochemical dynamics were controlled by an interplay of
30 meteorological conditions and geological heterogeneity. A principal component analysis

31 revealed that the largest variance (36.3 %) was explained by heavy metal concentrations (such
32 as Al, V, Cr, Ni, Zn, Cd, Pb) during the melting period while the remaining variance (16.3 %)
33 resulted from the bedrock type in the upper Sulden sub-catchment (inferred from electrical
34 conductivity, Ca, K, As and Sr concentrations). Thus, high concentrations of As and Sr in
35 rock glacier outflow may more likely result from bedrock weathering. Furthermore, nivo-
36 meteorological indicators such as daily maximum air temperature and daily maximum global
37 solar radiation represented important meteorological controls, with significant snowmelt
38 contribution when exceeding 5 °C or 1000 W m⁻², respectively. These insights may help to
39 better predict hydrochemical catchment responses linked to meteorological and geological
40 controls and to guide future classifications of glacierized catchments according to their
41 hydrochemical characteristics.

42

43 **1 Introduction**

44 Runoff from glacierized catchments is an important fresh water resource to downstream areas
45 (Kaser et al., 2010; Viviroli et al., 2011). High-elevation environments face rapid and
46 extensive changes through retreating glaciers, reduced snow cover, and permafrost thawing
47 (Harris et al., 2001; Dye, 2002; Beniston, 2003; Galos et al., 2015). This will have impacts on
48 runoff seasonality, water quantity and water quality (Beniston 2006; Ragettli et al., 2016;
49 Gruber et al., 2017). Therefore better understanding the behaviour of high-elevation
50 catchments and their hydrological and hydrochemical responses at different spatial and
51 temporal scales is of uttermost importance in view of water management, water quality,
52 hydropower, and ecosystem services under the current phase of climate change (Beniston,
53 2003; Viviroli et al., 2011; Beniston and Stoffel, 2014).

54 In general, the hydrological response of catchments (i.e., runoff dynamics) is controlled by
55 heterogeneous catchment properties (Kirchner, 2009), which become more diverse in
56 catchments with large complexity of various landscape features, as it is the case of
57 mountainous, high-elevation glacierized catchments (Cook and Swift, 2012). In fact, those
58 catchments are deemed as highly dynamic geomorphological, hydrological and
59 biogeochemical environments (Rutter et al., 2011). The advances on tracer and isotope
60 hydrology made during the last decades can substantially contribute to this objective, in order
61 to gain more insights into the variability of different runoff components (Vaughn and

62 Fountain, 2005; Maurya et al., 2011; Xing et al., 2015), catchment conceptualization (Baraer
63 et al., 2015; Penna et al., 2017), and sensitivity to climate change (Kong and Pang, 2012).

64 The main controls on hydrological and hydrochemical catchment responses are represented
65 by climate, bedrock geology, surficial geology, soil, vegetation, topography with drainage
66 network (Devito et al., 2005; Williams et al 2015) and catchment shape (Sivapalan 2003).

67 These catchment properties may affect the partitioning of incoming water and energy fluxes
68 (Carrillo et al., 2011).

69 First, a major role is attributed to the global and regional climate, having strong impacts on
70 mountain glaciers and permafrost, streamflow amount and timing, water quality, water
71 temperature, and suspended sediment yield (Milner et al., 2009; Moore et al., 2009; IPCC,
72 2013). The impact of climate is difficult to assess because it requires long time windows (e.g.,
73 decades), whereas meteorological drivers interact at a smaller temporal scales and thus are
74 easier to address. Among different meteorological drivers, radiation fluxes at the daily time
75 scale were identified as main energy source driving melting processes in glacierized
76 catchments in different climates (Sicart et al., 2008). Beside radiation, air temperature
77 variations generally correlate well with streamflow under the presence of snow cover (Swift et
78 al., 2005) and may affect streamflow seasonality only after a limiting value of air temperature
79 has been reached due to a threshold phenomena (Hock et al, 1999; Cortés et al., 2011).

80 Geology sets the initial conditions for catchment properties (Carrillo et al., 2011). The
81 geological setting strongly controls catchment connectivity, drainage, and groundwater
82 discharge (Farvolden 1963), runoff response (Onda et al., 2001), residence time (Katsuyama
83 et al., 2010), hydrochemistry during baseflow conditions (Soulsby et al., 2006a) and melting
84 periods (Hindshaw et al., 2011), and subglacial weathering (Brown and Fuge, 1998). Also
85 geomorphological features such as talus fields may affect streamflow and water quality,
86 resulting from different flow sources and flow pathways (Liu et al., 2004). Catchment storage,
87 as determined by both geology and topography, was found to impact the stream
88 hydrochemistry as well (Rinaldo et al., 2015).

89 The catchment hydrological conditions, commonly referring to the antecedent soil moisture,
90 are also a relevant driver of the hydrological response (Uhlenbrook and Hoeg, 2003; Freyberg
91 et al., 2017). Specifically in high elevation and high latitude catchments, also permafrost
92 thawing affects the hydrological connectivity (Rogger et al., 2017), leading to a strong control
93 on catchment functioning as it drives the partitioning, storage and release of water (Tetzlaff et

94 al., 2014). In more detail, retreating permafrost may also result in distinct geochemical
95 signatures (Clark et al., 2001; Lamhonwah et al., 2017) and the release of heavy metals being
96 previously stored in the ice (Thies et al., 2007; Krainer et al., 2015). Those contaminants do
97 not affect only the water quality but also the aquatic biota such as macroinvertebrate
98 communities in high elevation and high latitude environments (Milner et al., 2009). Different
99 weathering processes between the subglacial and periglacial environment can be found,
100 resulting in a shift in chemical species and concentrations in the water (Anderson et al., 1997).
101 Although the effect of catchment characteristics and environmental conditions on stream
102 hydrochemistry at different spatial and temporal scales has well been studied in lowland and
103 mid-land catchments (e.g. Wolock et al., 1997; McGuire et al. 2005; Tetzlaff et al., 2009),
104 only few studies have focused on this aspect in glacierized or permafrost-dominated
105 catchments (Wolfe and English, 1995; Hodgkins, 2001; Carey and Quinton 2005; Lewis et
106 al., 2012). In fact, investigating the geological, meteorological, and topographic controls on
107 catchment response and stream water hydrochemistry in high-elevation catchments is
108 essential when analyzing the origin of hydrochemical responses in larger catchments
109 (Chiogna et al., 2016; Natali et al., 2016), calibrating hydrological models (Weiler et al.,
110 2017) and analysing catchment storages (Staudinger et al., 2017).

111 In this context, also the hydrochemical characterization of permafrost thawing (i.e., from rock
112 glaciers as a specific form of permafrost) and its impact on stream hydrology deserves further
113 investigation (e.g. Williams et al., 2006, Carturan et al., 2015; Nickus et al. 2015; Colombo et
114 al. 2017)

115 In this paper, we aim to fill this gap by analysing hydrochemical data from a two year
116 monitoring campaign where samples for stable isotopes in water, electrical conductivity (EC),
117 turbidity, major, minor and trace elements analysis were collected for two nearby glacierized
118 catchments in the Eastern Italian Alps, characterized by similar size and climate but
119 contrasting geological setting.

120 Within the present study, we specifically aim to answer the following research questions:

- 121 • What is the role of geology on the hydrochemical stream signatures over time?
- 122 • Which are the most important nivo-meteorological indicators driving stream
123 hydrochemistry during the melting period?

- 124 • What is the temporal relationship of streamflow and tracer characteristics in the
125 stream?

126 **2 Study area and instrumentation**

127 **2.1 The Suldén River catchment**

128 The study was carried out in the Suldén/Soldá River catchment, located in the upper
129 Vinschgau/Venosta Valley (Eastern Italian Alps) (Fig. 1). The size of the study area is about
130 130 km² defined by the stream gauge station of the Suldén River at Stilsferbrücke/ Ponte
131 Stelvio (1110 m a.s.l.), with a mean elevation of 2507 m a.s.l.. The highest elevation is
132 represented by the Ortler/ Ortlers peak (3905 a.s.l.) within the Ortles-Cevedale group. A
133 major tributary is the Trafoi River, joining the Suldén River close to the village Trafoi-
134 Gomagoi. At this location, two sub-catchments, namely Suldén and Trafoi sub-catchment (75
135 and 51 km², respectively) meet.

136 The study area had a glacier extent of about 17.7 km² (14 % of the study area) in 2006, which
137 is slightly higher in the Trafoi than in the Suldén sub-catchment (17 % and 12 %, respectively).
138 Main glacier tongues in the study area are represented by the Madatsch glacier
139 (Trafoi sub-catchment) and Suldén glacier (Suldén sub-catchment). Geologically, the study
140 area belongs to the Ortler-Campo-Cristalin (Mair et al., 2007). While permotriassic
141 sedimentary rocks dominate the Trafoi sub-catchment, Quarzphyllite, Orthogneis, and
142 Amphibolit are present in the Suldén sub-catchment. However, both catchments share the
143 presence of orthogneis, paragneis and mica schist from the lower reaches to the outlet.
144 Permafrost is discontinuously located between 2400 and 2600 m a.s.l. and continuously above
145 2600 m a.s.l. (Boeckli et al., 2012). Available climatological data show a mean annual air
146 temperature is about -1.6 °C and the mean annual precipitation is about 1008 mm (2009 -
147 2016) at 2825 m a.s.l. (Hydrographic Office, Autonomous Province of Bozen-Bolzano). Due
148 to the location of the study area in the inner dry Alpine zone, these precipitation amounts are
149 relatively low compared to the amounts at similar elevation in the Alps (Schwarb, 2000).
150 Further climatic data regarding the sampling period of this study are shown in Table 1. The
151 study area lies within the National Park “Stelvio / Stilsfer Joch” but it also includes ski slopes
152 and infrastructures, as well as hydropower weirs.

153 **2.2 Meteorological, hydrometric and topographical data**

154 Precipitation, air temperature, humidity and snow depth are measured by an ultrasonic sensor
155 at 10 min measuring interval at the automatic weather station (AWS) Madritsch/Madriccio at
156 2825 m a.s.l., run by the Hydrographic Office, Autonomous Province of Bozen-Bolzano (Fig.
157 1). We take data from this station as representative for the glacier in the catchment at similar
158 elevation. At the catchment outlet at Stilfserbrücke/Ponte Stelvio, water stages are
159 continuously measured by an ultrasonic sensor (Hach Lange GmbH, Germany) at 10 min
160 measuring interval and converted to discharge via a flow rating curve using salt
161 dilution/photometric measurements (measurement range: $1.2 - 23.2 \text{ m}^3 \text{ s}^{-1}$; $n = 22$). Turbidity
162 is measured by a SC200 turbidity sensor (Hach Lange GmbH, Germany) at 5 min measuring
163 interval. EC is measured by a TetraCon 700 IQ (WTW GmbH, Germany) at 1 second
164 measuring interval. Both datasets were resampled to 10 min time steps. All data used in this
165 study are recorded and presented in solar time.

166 Topographical data (such as catchment area and 50 m elevation bands) were derived from a
167 2.5 m digital elevation model.

168 **2.3 Hydrochemical sampling and analysis**

169 Stream water sampling at the outlet was performed by an automatic sampling approach using
170 an ISCO 6712 system (Teledyne Technologies, USA). Daily water sampling took place from
171 mid-May to mid-October 2014 and 2015 (on 331 days) at 23:00 to ensure consistent water
172 sampling close to the discharge peak. In addition, grab samples from different stream
173 locations, tributaries, and springs in the Sulden and Trafoi sub-catchments and the outlet were
174 taken monthly from February 2014 to November 2015 (Table 2). Samples were collected
175 approximately at the same time (within less than an hour of difference) on all occasions. In
176 winter, however, a different sampling time had to be chosen for logistical constraints (up to
177 four hours of difference between both sampling times). However, this did not produce a bias
178 on the results due to the very limited variability of the hydrochemical signature of water
179 sources during winter baseflow conditions. Three outflows from two active rock glaciers were
180 selected to represent meltwater from permafrost because rock glaciers are considered as long
181 term creeping ice-rock mixtures under permafrost conditions (Humlum 2000). Located on
182 Quarzphyllite bedrock in the upper Sulden sub-catchment, three springs at the base of the

183 steep rock glacier front at about 2600 m a.s.l. were sampled monthly from July to September
184 2014 and July to October 2015. Snowmelt water was collected as dripping water from snow
185 patches from April to September 2014 and March to October 2015 (n = 48 samples), mainly
186 located on the west to north-facing slopes of the Sulden sub-catchment and at the head of the
187 valley in the Trafoi sub-catchment. Glacier melt water was taken from rivulets only at the
188 eastern tongue of the Sulden glacier from July to October 2014 and 2015 (n = 11 samples) for
189 its safe accessibility.

190 EC was measured in the field by a portable conductivity meter WTW 3410 (WTW GmbH,
191 Germany) with a precision of +/- 0.1 $\mu\text{S cm}^{-1}$ (nonlinearly corrected by temperature
192 compensation at 25 °C).

193 All samples were stored in 50 ml PVC bottles with a double cap and no headspace. The
194 samples were kept in the dark at 4°C in the fridge before analysis. $\delta^2\text{H}$ and $\delta^{18}\text{O}$ isotopic
195 composition of all water samples (except the ISCO stream water samples at the outlet) were
196 analysed at the Laboratory of Isotope and Forest Hydrology of the University of Padova
197 (Italy), Department of Land, Environments, Agriculture and Forestry by an off-axis integrated
198 cavity output spectroscopy (model DLT-100 908-0008, Los Gatos Research Inc., USA). The
199 analysis protocol and the description of reducing the carry-over effect are reported in (Penna
200 et al., 2010, 2012). The instrumental precision (as an average standard deviation of 2094
201 samples) is 0.5‰ for $\delta^2\text{H}$ and 0.08‰ for $\delta^{18}\text{O}$.

202 The $\delta^{18}\text{O}$ isotopic composition of the ISCO stream water samples was analysed by an isotopic
203 ratio mass spectrometer (GasBenchDelta V, Thermo Fisher) at the Free University of Bozen-
204 Bolzano. Following the gas equilibration method (Epstein and Mayeda, 1953), 200- μl sub-
205 samples were equilibrated with He-CO₂ gas at 23 °C for 18 h and then injected into the
206 analyser. The isotopic composition of each sample was calculated from two repetitions, and
207 the standard deviation was computed. The instrumental precision for $\delta^{18}\text{O}$ was $\pm 0.2\%$. We
208 applied a correction factor, described in Engel et al. (2016), to adjust the isotopic
209 compositions of $\delta^{18}\text{O}$ measured by the mass spectrometer to the ones measured by the laser
210 spectroscopy.

211 The analysis of major, minor and trace elements (Li, B, Na, Mg, Al, K, Ca, V, Cr, Mn, Fe,
212 Co, Ni, Cu, Zn, Rb, Sr, Mo, Ba, Pb and U) was carried out by Inductively Coupled Plasma

213 Mass Spectroscopy (ICP-MS ICAP-Q, Thermo Fischer) at the laboratory of EcoResearch srl.
214 (Bozen-Bolzano).

215 **2.4 Data analysis**

216 In order to better understand the effect of meteorological controls at different time scales,
217 different nivo-meteorological indicators derived from precipitation, air temperature, solar
218 radiation and snow depth data from AWS Madritsch, were calculated (Table 3).

219 We performed a temporal sensitivity analysis to better understand at which temporal scale
220 these nivo-meteorological indicators affect the hydrometric and hydrochemical stream
221 response at the outlet. For that purpose, we calculated the indicators for each day of stream
222 water sampling and included in the calculations a period of time of up to 30 days prior to the
223 sampling day by using a one day incremental time step. As precipitation indicators, we
224 considered the cumulated precipitation P in a period between 1 and 30 days prior to the
225 sampling day, and the period of time D_{prec} in days starting from 1, 10 or 20 mm of cumulated
226 precipitation occurred prior to the sampling day. We selected the daily maximum air
227 temperature T_{max} and daily maximum global solar radiation G_{max} in a period between 1 and 30
228 days prior the sampling day as snow and ice melt indicators. Moreover, we calculated the
229 difference of snow depth, ΔSD , and used it as as proxy for snowmelt. We derived this
230 indicator from measurements on the sampling day and the previous days, varying from 1 to 30
231 days. Then, we excluded snow depth losses up to 5 cm to remove noisy data. We also derived
232 the snow presence from these data when snow depth was exceeding 5 cm.

233 The temporal sensitivities of agreement between nivo-meteorological indicators and
234 hydrochemical signatures were expressed as Pearson correlation coefficients ($p < 0.5$) and
235 represented a measure to obtain the most relevant nivo-meteorological indicators to be
236 considered for further analysis in this study.

237 In order to understand the link among water sources and their hydrochemical composition, a
238 principle component analysis (PCA), using data centred to null and scaled to variance one (R
239 core team, 2016), was performed. Data below detection limit were excluded from the
240 analysis.

241 To assess the dampening effect of meltwater on stream water chemistry during baseflow
242 conditions and the melting period, the variability coefficient (VC) was calculated following
243 Eq. (1):

244 $VC = SD_{\text{baseflow}}/SD_{\text{melting}}$ (1)

245 where SD_{baseflow} is the standard deviation of stream EC sampled during baseflow conditions in
246 winter at a given location and SD_{melting} is the one at the same locations during the melt period
247 in summer (following Sprenger et al., 2016).

248 We applied a two-component mixing model based on EC and $\delta^2\text{H}$ data to separate the runoff
249 contributions originating from the Sulden and Trafoi sub-catchment at each sampling moment
250 during monthly sampling (Sklash and Farvolden, 1979), following Eq. (2) and Eq. (3):

251 $Q_{S1} = Q_{S2} + Q_{T1}$ (2)

252 $P_{T1} = (C_{S2} - C_{S1})/(C_{S2} - C_{T1})$ (3)

253 where P is the runoff proportion, C is the EC or isotopic composition in ^2H measured at the
254 locations S1 (outlet), S2 (sampling location in the Sulden sub-catchment upstream the
255 confluence with Trafoi River), and T1 (sampling location in the Trafoi sub-catchment
256 upstream the confluence with Sulden River, see Fig. 1). The uncertainty in the this calculation
257 was expressed as Gaussian error propagation using the instrumental precision of the
258 conductivity meter ($0.1 \mu\text{S cm}^{-1}$) and sample standard deviation from the laser spectroscopy,
259 following Genereux (1998). Furthermore, statistical analysis was performed to test the
260 variance of hydrochemical data by means of a t-test (if data followed normal distribution) or a
261 nonparametric Mann-Whitney Rank Sum test (in case of not-normally distributed data).

262 **3 Results**

263 **3.1 Origin of water sources**

264
265 To identify the geographic origin of stream water within the catchment, element
266 concentrations of stream and rock glacier spring water are presented in Table 4 and 5. It is
267 worth highlighting that heavy metal concentrations (such as Al, V, Cr, Ni, Zn, Cd, Pb)
268 showed highest concentrations during intense melting in July 2015 at all six locations (partly
269 exceeding concentration thresholds for drinking water (see European Union Drinking Water
270 Regulations 2014). Element concentrations were clearly higher at the most upstream sampling
271 locations. Relatively low variability coefficients ($VC < 0.3$) for these elements confirmed that
272 larger variations of concentrations occurred during the melting period and not during
273 baseflow conditions. Interestingly, the highest heavy metal concentrations (such as Mn, Fe,

274 Cu, Pb) of rock glacier springs SPR2 – 4 delayed the heavy metal concentration peak in the
275 stream by about two months.

276 In contrast, other element concentrations (such as As, Sr, K, Sb) generally revealed higher
277 concentrations during baseflow conditions and lower concentrations during the melting
278 period. This observation was corroborated by relatively high variability coefficients for As
279 (VC: 2 – 2.9) and Sb (VC: 2 – 2.2) at S1, S2, and T1. For example, while highest Sr
280 concentrations were measured at S6, As was highest at the downstream locations T1, S2, and
281 S1. Regarding the rock glacier springs, their hydrochemistry showed a gradual decrease in As
282 and Sr concentration from July to September 2015. The observed geochemical patterns are
283 confirmed by PCA results (Fig. 2) and the correlation matrix (Fig. 3), revealing that
284 geochemical dynamics are driven by temporal (PC1) and spatial controls (PC2) and a typical
285 clustering of elements, respectively. PC1 shows high loadings for heavy metal concentrations
286 (such as Al, V, Cr, Ni, Zn, Cd, Pb), supporting the clear temporal dependency for the entire
287 catchment (baseflow conditions vs. melting period)(Fig. 2a). PC2 is instead mostly
288 characterized by high loadings of $\delta^2\text{H}$ and $\delta^{18}\text{O}$ in the Trafoi sub-catchment (i.e. T1 and TT2)
289 and geochemical characteristics (EC, Ca, K, As and Sr) from the upstream region of the
290 Sulden River and rock glacier spring water (i.e. S6 and SSPR2-4, respectively). Overall,
291 temporal and spatial controls explained a variance of about 53 %.

292 **3.2 Temporal and spatial tracer variability in the sub-catchments**

293 The temporal and spatial variability of EC in the Sulden and Trafoi River along the different
294 sections, their tributaries, and springs is illustrated in Fig. 4. Results highlight the dominant
295 impact of water enriched in solutes during baseflow conditions starting from late autumn to
296 early spring prior to the onset of the melting period in May/June of both years. Such an
297 impact seemed to be highest in water from streams and tributaries reaching the most increased
298 conductivity at S6 during the study period compared to all sampled water types, ranging from
299 967 to 992 $\mu\text{S cm}^{-1}$ in January to March 2015. During the same period of time, isotopic
300 composition was slightly more enriched and spatially more homogeneous among the stream,
301 tributaries, and springs than in the summer months. In contrast, during the melting period,
302 water from all sites in both sub-catchments became diluted due to different inputs of
303 meltwater (Fig. 4a, b), while water was most depleted during snowmelt dominated periods
304 (e.g., mid-June 2014 and end of June 2015) and less depleted during glacier melt dominated

305 periods (e.g., mid to end of June 2014 and 2015) (Fig. 4c and 4d). Rainfall became a
306 dominant runoff component during intense storm events. For instance, on 24 September 2015,
307 a storm of 35 mm d⁻¹ resulted in the strongest isotopic enrichment of this study, which is
308 visible in Fig. 4c at T3 and TT2 ($\delta^2\text{H}$ -86.9 ‰; $\delta^{18}\text{O}$: -12.4 ‰).

309 Hereinafter, the hydrochemistry of the Sulden and Trafoi sub-catchment is analyzed in terms
310 of hydrochemical patterns of the main stream, tributaries, springs, and runoff contributions at
311 the most downstream sampling location above the confluence. At T1 and S2, hydrochemistry
312 was statistically different in its isotopic composition (Mann-Whitney Rank Sum Test: $p <$
313 0.001) but not in EC (Mann-Whitney Rank Sum Test: $p = 0.835$). Runoff originating from
314 Trafoi and derived from the two-component HS, contributed to the outlet by about 36 %
315 (± 0.004) to 58 % (± 0.003) when using EC and ranged from 29 % (± 0.09) to 83 % (± 0.15)
316 when using $\delta^2\text{H}$. Streamflow contributions expressed as specific discharge from Trafoi sub-
317 catchment (Sulden sub-catchment) were 20.6 (37.1) and 16.2 (12) l s⁻¹ km² for EC and 50.4
318 (121.9) and 12.2 (2.6) l s⁻¹ km² for $\delta^2\text{H}$. Therefore, with respect to the temporal variability of
319 the sub-catchment contributions, runoff at the outlet was sustained more strongly by the
320 Trafoi River during non-melting periods while the runoff from the Sulden sub-catchment
321 dominated during the melting period.

322 By the aid of both tracers, catchment specific hydrochemical characteristics such as
323 contrasting EC gradients along the stream were revealed (Fig. 4 and Fig. 5). EC in the Trafoi
324 River showed linearly increasing EC with increasing catchment area (from T3 to T1) during
325 baseflow and melting periods ('EC enrichment gradient').

326 In contrast, the Sulden River revealed relatively high EC at the highest upstream location (S6)
327 and relatively low EC upstream the confluence with the Trafoi River (S2) during baseflow
328 conditions. The exponential decrease in EC ('EC dilution gradient') during this period of time
329 was strongly linked to the catchment area. Surprisingly, the EC dilution along the Sulden
330 River was still persistent during melting periods but highly reduced. In this context, it is also
331 interesting to compare the EC variability (expressed as VC) along Trafoi and Sulden River
332 during baseflow conditions and melting periods (Table 6). For both streams, VC increased
333 with decreasing distance to the confluence (Trafoi River) and the outlet (Sulden River), and
334 thus representing an increase in catchment size. The highest EC variability among all stream
335 sampling locations is given by the lowest VC, which was calculated for S6. This location

336 represents the closest one to the glacier terminus and showed a pronounced contrast of EC
337 during baseflow conditions and melting periods (see Fig. 4 and Fig. 5).
338 Regarding the hydrochemical characterisation of the tributaries in both sub-catchments (Fig.
339 4), Sulden tributaries were characterised by a relatively low EC variability (68.2 – 192.3
340 $\mu\text{S cm}^{-1}$) and more negative isotopic values ($\delta^2\text{H}$: -100.8 – 114.5 ‰) compared to the higher
341 variability in hydrochemistry of the Sulden River. In contrast, the tracer patterns of Trafoi
342 tributaries were generally consistent with the ones from the stream. Generally, also spring
343 water at TSPR1, TSPR2, and SSPR1 followed these patterns during baseflow and melting
344 periods in a less pronounced way, possibly highlighting the impact of infiltrating snowmelt
345 into the ground. Comparing both springs sampled in the Trafoi sub-catchment indicated that
346 spring waters were statistically different only when using EC (Mann-Whitney Rank Sum
347 Test: $p = 0.039$). While TSPR1 hydrochemistry was slightly more constant, the one of TSPR2
348 was more variable from June to August 2015 (Fig. 4).

349 **3.3 Meteorological controls on hydrometric and hydrochemical stream responses at** 350 **the catchment outlet**

351 To identify the effect of meteorological controls at high elevation on the hydrometric and
352 hydrochemical stream response at the outlet, we first present the relationship between
353 meteorological parameters against snow depth differences (Fig. 6). Then, we show snow
354 depth differences compared with discharge, EC and isotopic data (Fig. 7).

355 Among the nivo-meteorological indicators listed in Table 3, daily maximum air temperature
356 T_{max} and daily maximum global solar radiation G_{max} were the most important drivers to
357 control snowmelt (expressed as snow depth differences) at high elevation (Fig. 6). While
358 moderate snow depths losses by up to 30 cm occurred during days with T_{max} between 0 and
359 5 °C, higher snow depths losses of 30 to 80 cm were associated with warmer days, when T_{max}
360 ranged between 5 °C and 12.5 °C at AWS Madritsch.

361 With respect to G_{max} , only small snow depth losses of up to 10 cm and small variability were
362 present when G_{max} ranged from 600 to 1000 W m^{-2} . As soon as the daily maximum of 1000
363 W m^{-2} was passed, snow depth losses could reach a maximum of up to 80 cm. When
364 exceeding these T_{max} and G_{max} thresholds, the variability of snow depth losses remarkably
365 increased and was larger the longer the time scale of the observation period was (i.e. 8 – 14
366 days).

367 As a consequence, high elevation snowmelt played an important role in explaining both the
368 hydrometric and hydrochemical response at the outlet Stilsferbrücke (Fig. 7). During the
369 snowmelt period, discharge at the outlet clearly increased with increasing snowmelt due to
370 snow depth losses at high elevation. For example, median discharges of 6.25 and 7.5 m³ s⁻¹
371 resulted from snow depth losses of 50 and 75 cm while discharges higher than 20 m³ s⁻¹
372 occurred when snow depth losses were higher than 100 cm during the previous days.
373 Moreover, the increasing amount of snowmelt resulted in decreasing EC and lower δ¹⁸O.
374 While median EC of about 250 μS cm⁻¹ was still relatively high after snow depth losses
375 between 50 and 75 cm occurred, highest losses induced a drop in EC of about 50 μS cm⁻¹.
376 With respect to the same snow depth losses, median stream water δ¹⁸O reached -13.8 ‰ and
377 ranged between -14.1 and -14.3 ‰, respectively. However, due to higher variability of δ¹⁸O,
378 the effect of snowmelt water on the isotopic composition was less clear than the dilution
379 effect on EC.

380 **3.4 Temporal variability at the catchment outlet**

381 The temporal variability of the hydrochemical variables observed at the catchment outlet and
382 of the meteorological drivers is illustrated in Fig. 8. Controlled by increasing radiation inputs
383 and air temperatures above about 5°C in early summer (Fig. 6, Fig. 7, Fig. 8a and 8b), first
384 snowmelt (as indicated by an EC of about 200 μS cm⁻¹ and a depleted isotopic signature of
385 about -14.6 ‰ in δ¹⁸O) induced runoff peaks in the Suldner River of about 20 m³ s⁻¹ (starting
386 from a winter baseflow of about 1.8 m³ s⁻¹), as shown in Fig. 8c and 8e. In comparison, the
387 average snowmelt EC was 28 μS cm⁻¹ and -14.84 in δ¹⁸O. Later in the summer, glacier melt
388 induced runoff peaks reached about 13 – 18 m³ s⁻¹, which are characterised by relatively low
389 EC (about 235 μS cm⁻¹) and isotopically more enriched stream water (δ¹⁸O: about -13.3 ‰).
390 In fact, glacier melt showed an average EC of 36.1 μS cm⁻¹ and average of 13.51 ‰ in δ¹⁸O.
391 The highest discharge measured during the analysed period (81 m³ s⁻¹ on 13 August 2014)
392 was caused by a storm event, characterized by about 31 mm of precipitation falling over 3
393 hours at AWS Madritsch. Unfortunately, isotopic data for this event were not available due to
394 a technical problem with the automatic sampler.

395 Water turbidity was highly variable at the outlet, and mirrored the discharge fluctuations
396 induced by meltwater or storm events. Winter low flows are characterised by very low

397 turbidity (< 10 NTU, corresponding to less than 6 mg l^{-1}). In summer, turbidity ranged
398 between 20 and up to 1200 NTU during cold spells and melt events combined with storms,
399 respectively. However, the maximum value recorded was 1904 NTU reached after several
400 storm events of different precipitation amounts (17 mm, 50 mm, and 9 mm) on 12, 13, and 14
401 August 2014, respectively. Unfortunately, the turbidimeter did not work properly after the
402 August 2014 flood peak, in mid-July 2015 and beginning of October 2015.

403 Furthermore, the interannual variability of meteorological conditions with respect to the
404 occurrence of warm days, storm events and snow cover of the contrasting years 2014 and
405 2015 is clearly visible and contributed to the hydrochemical dynamics (Fig.8 and Table 1).
406 While about 250 cm of maximal snowpack depth in 2014 lasted until mid-July, only about
407 100 cm were measured one year after with complete disappearance of snow one month
408 earlier. In 2015, several periods of remarkable warm days occurred reaching more than 15°C
409 at 2825 m a.s.l. and led to a catchment entirely under melting conditions (freezing level above
410 5000 m a.s.l., assuming a lapse rate of $6.5^{\circ}\text{C km}^{-1}$). In contrast, warmer days in 2014 were
411 less pronounced and frequent but accompanied by intense storms of up to 50 mm d^{-1} . These
412 meteorological conditions seem to contribute to the general hydrochemical patterns described
413 above. Despite a relatively similar hydrograph with same discharge magnitudes during melt-
414 induced runoff events in both years, EC and $\delta^{18}\text{O}$ clearly characterized snowmelt and glacier
415 melt-induced runoff events in 2014. However, a characteristic period of depleted or enriched
416 isotopic signature was lacking in 2015 so that snowmelt and glacier melt-induced runoff
417 events were graphically more difficult to distinguish.

418 The daily variations in air temperature, discharge, turbidity, and EC showed marked
419 differences in the peak timing. Daily maximum air temperature generally occurred between
420 12:00 and 15:00, resulting in discharge peaks at about 22:00 to 1:00 in early summer and at
421 about 16:00 to 19:00 during late summer. Turbidity peaks were measured at 22:00 to 23:00 in
422 May to June and distinctively earlier at 16:00 to 19:00 in July and August. In contrast, EC
423 maximum occurred shortly after the discharge peak between 00:00 to 1:00 in early summer
424 and at 11:00 to 15:00, clearly anticipating the discharge peaks.

425 It is interesting to highlight a complex hydrochemical dynamics during the baseflow period in
426 November 2015, which was interrupted only by a rain-on-snow event on 28 and 29 October
427 2015. This event was characterized by more liquid (12.9 mm) than solid precipitation
428 (6.6 mm) falling on a snowpack of about 10 cm (at 2825 m a.s.l.). While stream discharge

429 showed a typical receding hydrograph confirmed by EC being close to the background value
430 of about $350 \mu\text{S cm}^{-1}$, $\delta^{18}\text{O}$ indicated a gradual isotopic depletion suggesting the occurrence
431 of isotopically depleted water (e.g., snowmelt) in the stream. Indeed, also turbidity was more
432 variable and slightly increased during this period.

433 To better characterize the temporal dynamics of hydrochemical variables, Fig. 9 shows the
434 different relationships of discharge, EC, $\delta^{18}\text{O}$, and turbidity grouped for different months. In
435 general, high turbidity was linearly correlated with discharge showing a monthly trend (Fig.
436 9a). This observation could be explained by generally higher discharges during melting
437 periods (June, July, and August) and lower ones during baseflow conditions. Discharge and
438 EC exhibited a relationship characterised by a hysteretic-like pattern at the monthly scale
439 (Fig. 9b), which was associated with the monthly increasing contribution of meltwater with
440 lower EC during melting periods contrasting with dominant groundwater contributions having
441 higher EC during baseflow conditions.

442 During these periods, $\delta^{18}\text{O}$ of stream water was mainly controlled by the dominant runoff
443 components (i.e., snowmelt and glacier melt in early summer and mid- to late summer,
444 respectively) rather than the amount of discharge (Fig. 9c). Similarly, the relationship
445 between $\delta^{18}\text{O}$ and EC was driven by the discharge variability resulting in a specific range of
446 EC values for each month and by the meltwater component generally dominant during that
447 period (Fig. 9d). As $\delta^{18}\text{O}$ was dependent on the dominant runoff components and less on the
448 amount of discharge, turbidity showed no clear relationship with the isotopic composition
449 (Fig. 9e). In contrast, EC and turbidity were controlled by monthly discharge variations so
450 that both variables followed the monthly trend, revealing a linear relationship (Fig. 9f).

451 Finally, as the hysteretic-like pattern of discharge and EC was the strongest relationship
452 obtained, we evaluated this pattern in more detail and compared it against T_{max} , G_{max} and the
453 snow presence (Fig. 10). While T_{max} at high elevation ranged between 0 and 5 °C and G_{max}
454 already exceeded 1000 W m^{-2} during early summer, increasing discharge with decreasing EC
455 was observed at the outlet. This pattern progressed further as more snowmelt was available
456 due to T_{max} increasing to 5 to 10 °C and high G_{max} . Interestingly, highest discharges with
457 lowest EC occurred during days with $G_{\text{max}} > 1300 \text{ W m}^{-2}$ but not during the warmest days
458 when snowcover at high elevation was both present and absent. Thus, runoff events during
459 this period of time were clearly snowmelt and glacier melt-induced, also because only one

460 storm event of $P_{1d} = 12.2$ mm was measured. In late summer and autumn, discharges started
461 to fall while EC increased during snow-free days with decreasing T_{max} but still high G_{max} . As
462 soon as T_{max} was below 5°C , discharges dropped below $10 \text{ m}^3 \text{ s}^{-1}$ and EC rose above 250
463 $\mu\text{S cm}^{-1}$, characterizing the initial phase of baseflow conditions in the Sulden River.

464

465 **4 Discussion**

466 **4.1 Geological controls on the stream hydrochemistry**

467 Hydrochemical dynamics were driven by a pronounced release of heavy metals (such as Al,
468 V, Cr, Ni, Zn, Cd, Pb) shown for the entire catchment and, in contrast, by a specific release of
469 As and Sr in the upper and lower Sulden sub-catchment (Fig. 2). Yet, as the explained
470 variance was only at about 53 %, further controls may be present. In this context, PC3
471 explained 11.8% of additional variance and may characterize the hydrochemistry of surface
472 and subsurface flows resulting from different residence times within the different soils and
473 rocks.

474 With respect to PC1, several sources of heavy metals can be addressed: these elements may
475 be released by rock weathering on freshly-exposed mineral surfaces and sulphide oxidation,
476 typically produced in metamorphic environments (Nordstrom et al., 2011). Proglacial stream
477 hydrochemistry may also strongly depend on the seasonal evolution of the subglacial drainage
478 system that contribute to the release of specific elements (Brown and Fuge, 1998). In this
479 context, rock glacier thawing may play an important role for the release of Ni (Thies et al.,
480 2007; Mair et al., 2011; Krainer et al., 2015) and Al and Mn (Thies et al., 2013). However,
481 high Ni concentrations were not observed in this study. Moreover, high heavy metal
482 concentrations were measured during the melting period in mid-summer, which would be
483 generally too early to derive from permafrost thawing (Williams et al., 2006; Krainer et al.,
484 2015). Also bedrock weathering as major origin probably needs to be excluded because low
485 concentrations of heavy metals occurred in winter when the hydrological connectivity at
486 higher elevations was still present (inferred from running stream water at the most upstream
487 locations).

488 It is therefore more likely that heavy metals derive from meltwater itself due to the spatial and
489 temporal dynamics observed. This would suggest that the element release is strongly coupled

490 with melting and infiltration processes, when hydrological connectivity within the catchment
491 is expected to be highest. To support this explanation, supplementary element analysis of
492 selected snowmelt ($n = 2$) and glacier melt ($n = 2$) samples of this study were conducted.
493 Although these samples did not contain high concentrations of Cd, Ni, and Pb, snowmelt in
494 contact with the soil surface was more enriched in such elements than dripping snowmelt.
495 Moreover, in a previous study in the neighbouring Matsch/Mazia Valley in 2015, snowmelt
496 and ice melt samples were strongly controlled by high Al, Co, Cd, Ni, Pb and Zn
497 concentrations (Engel et al., 2017). As shown for 21 sites in the Eastern Italian Alps (Veneto
498 and Trentino-South Tyrol region), hydrochemistry of the snowpack can largely be affected by
499 heavy metals originating from atmospheric deposition from traffic and industry (such as V,
500 Sb, Zn, Cd, Mo, and Pb) (Gabrielli et al., 2006). Likely, orographically induced winds and
501 turbulences arising in the Alpine valleys may often lead to transport and mixing of trace
502 elements during winter. Studies from other regions, such as Western Siberia Lowland and the
503 Tibetan Plateau, agree on the anthropogenic origin (Shevchenko et al., 2016 and Guo et al.,
504 2017, respectively).

505 In contrast, a clear geological source can be attributed to the origin of As and Sr, indicating a
506 bedrock-specific geochemical signatures. In the lower Sulden catchment (i.e. S1, S2, and T1),
507 As could mainly originate from As-containing bedrocks. As rich lenses are present in the
508 cataclastic carbonatic rocks (realgar bearing) and in the mineralized, arsenopyrite bearing
509 bands of quartzphyllites, micaschists and paragneisses of the crystalline basement. Different
510 outcrops and several historical mining sites are known and described in the literature (Mair,
511 1996, Mair et al., 2002, 2009; Stingl and Mair, 2005). In the upper Sulden catchment, the
512 presence of As is supported by the hydrochemistry of rock glacier outflows in the Zay sub-
513 catchment (corresponding to the drainage area of ST2; Engel et al., 2018) but was not
514 reported in other studies (Thies et al., 2007; Mair et al., 2011; Krainer et al., 2015; Thies et
515 al., 2013). Also high-elevation spring waters in the Matsch Valley corroborated that As and Sr
516 concentrations may originate from paragneisses and micaschists (Engel et al., 2017).
517 However, the gradual decrease in As and Sr concentrations from rock glacier springs clearly
518 disagrees with the observations from other studies that rock glacier thawing in late summer
519 leads to increasing element releases (Williams et al., 2006; Thies et al., 2007; Krainer et al.,
520 2015; Nickus et al., 2015). We suggest a controlling mechanism as follows: it is more likely
521 that As and Sr originate from the Quarzphyllite rocks, that form the bedrock of the rock

522 glaciers (see Andreatta, 1952; Montrasio et al., 2012). Weathering and former subglacial
523 abrasion facilitate this release (Brown, 2002). As- and Sr-rich waters may form during winter
524 when few quantities of water percolate in bedrock faults and then are released due to
525 meltwater infiltration during summer (V. Mair, personal communication, 2018). As a clear
526 delayed response of heavy metal concentrations in rock glacier outflow was revealed, the
527 infiltration and outflow processes along flow paths in the bedrock near the rock glaciers may
528 take up to two months to hydrochemically respond to snowmelt contamination.

529 As a consequence, a clear hydrochemical signature of permafrost thawing is difficult to find
530 and results may lack the transferability to other catchments as not all rock glaciers contain
531 specific elements to trace (Colombo et al., 2017). In this context, as precipitation and
532 snowmelt affect the water budget of rock glaciers (Krainer and Mostler, 2002; Krainer et al.,
533 2007), potential impacts of atmospheric inputs on rock glacier hydrochemistry could be
534 assumed and would deserve more attention in future (Colombo et al., 2017).

535 Furthermore, export of elements in fluvial systems is complex and may strongly be affected
536 by the pH (Nickus et al., 2015) or interaction with solids in suspension (Brown et al., 1996),
537 which could not be addressed in this study. Further insights on catchment processes might be
538 gained considering also element analysis of the solid fraction, to investigate whether water
539 and suspended sediment share the same provenance.

540 **4.2 The role of nivo-meteorological conditions**

541 Superimposing the impact of the geological origin, melting processes were controlled by
542 meteorological conditions, affecting stream hydrochemistry during summer, as shown by
543 isotope dynamics (Fig. 4 and 8) and hydrochemical relationships (Fig. 9). It is well known
544 that snowmelt is mainly driven by radiation and temperature. Generally, radiation is the main
545 energy source driving melt processes in glacierized catchments of different climates (Sicart et
546 al., 2008; Vincent and Six (2013) and may integrate the effect of cloud coverage (Anslow et
547 al., 2008). Moreover, it exists a high correlation between snow or glacier melt and maximum
548 air temperature (U.S. Army Corps of Engineers 1956; Braithwaite 1981), thus controlling
549 daily meltwater contributions to streamflow (Mutzner et al., 2015; Engel et al., 2016). T_{\max} is
550 widely used for characterizing snow transformation processes such as the decay of snow
551 albedo and snow metamorphism (e.g., Ragetti and Pellicciotti, 2012).

552 In this study, we show that T_{\max} of about 5 °C and G_{\max} of about 1000 W m⁻² may represent
553 important meteorological thresholds to trigger pronounced snow depth losses and thus
554 snowmelt in the study area and other high-elevation catchments. In agreement with our
555 findings, Ragetti and Pellicciotti (2012) used the same 5°C threshold temperature for melt
556 onset (as shown in Fig. 6a and Fig. 8).

557 Of course, further nivo-meteorological indicators such as the extent of snow cover (Singh et
558 al., 2005), vapour pressure, net radiation, and wind (Zuzel and Cox, 1975) or turbulent heat
559 fluxes and long-wave radiation (Sicart et al., 2006) may exist but were not included in the
560 present study due to the lack of observations.

561 Moreover, with respect to spatial representativeness, T_{\max} and G_{\max} represent point-scale data
562 from the only high-elevation AWS of this catchment, providing the nivo-meteorological
563 indicators needed for this study. However, not only elevation controls snowmelt but also
564 spatial variability of other factors such as aspect, slope, and microtopography (e.g., Anderton
565 et al. 2002; Grünwald et al. 2010; Lopez-Moreno et al. 2013), which could not be addressed
566 here. These site characteristics usually lead to different melt rates and thus affect the isotopic
567 snowmelt signature (Taylor et al. 2001; Taylor et al. 2002; Dietermann and Weiler, 2013) and
568 the hydrometric response in the main channel such as the timing of the discharge peak
569 (Lundquist and Dettinger, 2005).

570 The temporal sensitivity analysis and the relatively large variability related to snow depth
571 losses (Fig. 6 and Fig. 7) are generally difficult to compare due to the lack of suitable studies.
572 Moreover we considered ΔSD of up to 5cm as noisy data, but we did not discard data when
573 strong winds occurred, likely resulting in pronounced blowing snow. In addition, decreasing
574 snow depth may be the result of undergoing snow compaction, not related to the release of
575 melt water from the snowpack. Therefore, the use of snow depth losses as proxy for snowmelt
576 has to be considered with care.

577 The contrasting variabilities of discharge, EC, and $\delta^{18}O$ with respect to the observed time
578 scale (Fig. 7) may also result from different flow paths and storages in the catchment, such as
579 the snowpack itself as short-term storage for meltwater ranging from few hours to few days
580 (Coléou and Lesaffre, 1998). Slower and quicker flow paths within glacial till, talus,
581 moraines, and shallow vs. deeper groundwater compartments could indicate intermediate and
582 longer (14 days) meltwater response (Brown et al., 2006; Roy and Hayashi, 2009;
583 McClymont et al., 2010; Fischer et al., 2015; Weiler et al., 2017).

584 4.3 Implications for streamflow and hydrochemistry dynamics

585 Tracer dynamics of EC and stable isotopes associated with monthly discharge variations
586 generally followed the conceptual model of the seasonal evolution of streamflow
587 contributions, as described for catchments with a glacierized area of 17 % (Penna et al. 2017)
588 and 30 % (Schmieder et al. 2017). However, isotopic dynamics were generally less
589 pronounced compared to these studies, likely resulting from the impact of relative meltwater
590 contribution related to different catchment sizes and the proportion of glacierized area (Baraer
591 et al., 2015).

592 In addition, hydrometric and geochemical dynamics analysed in this study were controlled by
593 an interplay of meteorological conditions and the heterogeneity of geology. Such an interplay
594 is highlighted by EC dynamics (i.e., EC variability derived from VC), to be further controlled
595 by the contributing catchment area (i.e. EC gradients along the Sulden and Trafoi River)
596 (Wolock et al., 1997; Peralta-Tapia et al. 2015; Wu 2018). As EC was highly correlated to Ca
597 concentration (Spearman rank correlation: 0.6, $p < 0.05$; see Fig. 3), EC dynamics were
598 determined by the spatial distribution of different geology. For example, as dolomitic rocks
599 are present almost within the entire Trafoi sub-catchment, meltwater following the hydraulic
600 gradient can likely become more enriched in solutes with longer flow pathways and
601 increasing storage capability related to the catchment size (Fig. 5). As consequence, the 'EC
602 enrichment gradient' could persist during both the melting period and baseflow conditions in
603 the presence of homogenous geology. Therefore, topography may become a more important
604 control on spatial stream water variability than the geological setting. In the Sulden sub-
605 catchment, however, dolomitic rocks are only present in the upper part of the catchment while
606 metamorphic rocks mostly prevail. This leads to a pronounced dilution during baseflow
607 conditions of Ca-rich waters with increasing catchment area or in other words, increasing
608 distance from the source area (Fig. 5). This implies that meltwater contributions to the stream
609 homogenize the effect of geographic origin on different water sources, having the highest
610 impact in vicinity of the meltwater source (see Table 6).

611 The additional effect of topographical characteristics is underlined by the findings that the
612 Sulden River hydrochemistry at S2 was significantly more depleted in $\delta^2\text{H}$ and $\delta^{18}\text{O}$ than T1
613 hydrochemistry. Compared with the Sulden sub-catchment, the Trafoi sub-catchment has a
614 slightly lower proportion of glacier extent but, more importantly, has a clearly smaller

615 catchment area within the elevation bands of 1800 to 3200 m a.s.l. (i.e. 40.2 km² for the
616 Trafoi and 66.5 km² for the Sulden sub-catchment). In this elevation range, the sub-
617 catchments of major tributaries ST1, ST2, and ST3 are situated, which deliver large snowmelt
618 contributions to the Sulden River (Fig. 4 and Fig. 5).

619 In consequence, meteorological conditions, geology and topography explain specific
620 hydrometric and hydrochemical relationships at the catchment outlet. For example, the
621 hysteretic relationship between discharge and EC (Fig. 8b) corresponds well with the
622 hysteresis observed in the nearby Saldur and Alta Val de La Mare catchment (Engel et al.,
623 2016; Zuecco et al. 2016), although these studies focused on the runoff event scale. The initial
624 phase of this hysteresis in early summer was clearly snowmelt-induced with snowmelt likely
625 originating from lower elevations as T_{\max} at high elevation was still relatively low (0 – 5°C).
626 The further development of the hysteresis is then linked to the progressing snowmelt
627 contribution towards higher elevations. In contrast, the phase of hysteresis in late summer to
628 early autumn is determined by glacier melt and its decreasing contributions when low T_{\max}
629 and G_{\max} indicate the lack of available energy for melting.

630 Moreover, this relationship helps to identify the conditions with maximum discharge and EC:
631 during baseflow conditions, the Sulden River showed highest EC of about 350 $\mu\text{S cm}^{-1}$
632 seemingly to be bound to only about 3 $\text{m}^3 \text{s}^{-1}$ whereas the maximum dilution effect occurred
633 during a storm on 29 June 2014 (55 mm of precipitation at AWS Madritsch) with 29.3 $\text{m}^3 \text{s}^{-1}$
634 of discharge resulting in only 209 μScm^{-1} . However, these observations based on daily data
635 sampled at 23:00, likely not capturing the entire hydrochemical variability inherent of the
636 Sulden catchment. As shown in Fig. 5 and Fig. 7, much higher discharges and thus even lower
637 EC could be reached along the Sulden River and inversely, which was potentially limited by
638 the specific geological setting of the study area.

639 As more extreme weather conditions (such as heat waves, less solid winter precipitation) are
640 expected in future (Beniston, 2003; Viviroli et al., 2011; Beniston and Stoffel 2014),
641 glacierized catchments may exhibit more pronounced hydrochemical responses such as
642 shifted or broader ranges of hydrochemical relationships and increased heavy metal
643 concentrations both during melting periods and baseflow conditions. However, identifying
644 these relationships with changing meteorological conditions would deserve more attention
645 and is strongly limited by our current understanding of underlying hydrological processes
646 (Schaeffli et al., 2007). In a changing cryosphere, more complex processes such as non-

647 stationarity processes may emerge under changing climate, which was found to be a major
648 cause of non-stationarity (Milly et al., 2008). In this context, explaining apparently ambiguous
649 processes as the one we observed during the baseflow period in November 2015 (Fig. 8) will
650 deserve further attention.

651 Finally, our results underline that long-term controls such as geology and topography govern
652 hydrochemical spatial responses (such as bedrock-specific geochemical signatures, EC
653 gradients, and relative snowmelt contribution). In contrast, short-term controls such as daily
654 maximum solar radiation, air temperature, and snow depth differences drive short-term
655 responses (such as discharge variability and EC dilution). Both statements are in general
656 agreement with the findings of Heidbüchel et al. (2013). However, as the catchment response
657 strongly depended on the melting period vs. baseflow conditions, controls at longer temporal
658 scales interact as well. Thus, our findings suggest that glacierized catchments react in a much
659 more complex way and that catchment responses cannot be attributed to one specific scale,
660 justified by either short-term or long-term controls alone.

661 In this context, the present study provides novel insights into geological, meteorological, and
662 topographic controls of stream water hydrochemistry rarely addressed for glacierized
663 catchments so far. Moreover, this study strongly capitalizes on an important dataset that
664 combines nivo-meteorological indicators and different tracers (stable isotopes of water, EC,
665 major, minor and trace elements), underlining the need for conducting multi-tracer studies in
666 complex glacierized catchments.

667 **4.4 Methodological limitation**

668 The sampling approach combined a monthly spatial sampling with daily sampling at the
669 outlet, which methodologically is in good agreement with other sampling approaches,
670 accounting for increasing distance of sampling points to the glacier (Zhou et al., 2014; Baraer
671 et al., 2015), intense spatial and temporal sampling (Penna et al., 2014; Fischer et al., 2015),
672 synoptic sampling (Carey et al., 2013; Gordon et al., 2015), and different catchment structures
673 such as nested catchments (Soulsby et al., 2006b). Sampling covered a variety of days with
674 typical snowmelt, glacier melt and baseflow conditions during 2014 and 2015, confirming the
675 representativeness of tracer dynamics within two years with contrasting meteorological
676 characteristics (Table 1). However, short-term catchment responses (such as storm-induced
677 peak flows and related changes in hydrochemistry) were difficult to capture by this sampling

678 approach. In this context, also the representativeness of the outlet sampling time with respect
679 to the peak discharge time at that location may play an important role. In fact, the peak of
680 hydrochemical response may not be synchronized with the hydrometric one and therefore
681 may lead to stronger or weaker relationships.

682 Furthermore, two years of field data are probably not sufficient to capture all hydrological
683 conditions and catchment responses to specific meteorological conditions. In this regards,
684 long-term studies may have better chances in capturing the temporal variability of
685 hydrochemical responses (Thies et al., 2007). Although time-, energy- and money-consuming,
686 more complex and long sampling approaches should be developed to further unravel process
687 understanding of glacierized catchments.

688

689 **5 Conclusions**

690 Our results highlight the complex hydrochemical responses of mountain glacierized
691 catchments at different temporal and spatial scales. To our knowledge, only few studies
692 investigated the impact of controlling factors on stream water hydrochemistry by using nivo-
693 meteorological indicators and multi-tracer data, which we recommend to establish as
694 prerequisite for studies in other glacierized catchments.

695 The main results of this study can be summarized as follows:

- 696 • Hydrometric and geochemical dynamics were controlled by an interplay of
697 meteorological conditions and the geological heterogeneity. The majority of the
698 variance (PC1: 36.3 %) was explained by heavy metal concentrations (such as Al, V,
699 Cr, Ni, Zn, Cd, Pb), associated with atmospheric deposition on the snowpack and
700 release through snowmelt. Remaining variance (PC2: 16.3 %) resulted both from the
701 presence of a bedrock-specific geochemical signature (As and Sr concentrations) and
702 the role of snowmelt contribution.
- 703 • The isotopic composition of rock glacier outflow was relatively similar to the
704 composition of glacier melt whereas high concentrations of As and Sr may more likely
705 result from bedrock weathering. Therefore, as the underlying geology may prevails
706 over a thawing permafrost characteristics, a specific hydrochemical signature of rock
707 glacier springs was difficult to obtain.

- 708 • At the monthly scale for different sub-catchments (spatial scale: 0.05 – 130 km²), both
709 $\delta^{18}\text{O}$ and EC revealed complex spatial and temporal dynamics such as contrasting EC
710 gradients during baseflow conditions and melting periods.
- 711 • At the daily scale for the entire study area (spatial scale: 130 km²), we observed strong
712 relationships of hydrochemical variables, with mainly discharge and EC exhibiting a
713 strong monthly relationship. This was characterised by a hysteretic-like pattern,
714 determined by highest EC and lowest discharge during baseflow conditions and
715 maximum EC dilution due to highest discharge during a summer storm.
- 716 • Daily maximum air temperature T_{max} and daily maximum global solar radiation G_{max}
717 were the most important drivers to control snowmelt at high elevation. T_{max} of about
718 5 °C and G_{max} of about 1000 W m⁻² may represent meteorological thresholds to trigger
719 pronounced snow depth losses and thus snowmelt in the study area. However, the use
720 of snow depth losses as proxy for snowmelt has to be considered with care due to
721 uncertainties related to blowing snow or snow compaction without meltwater outflow.

722

723 Finally, this study may support future classifications of glacierized catchments according to
724 their hydrochemical response under different catchment conditions or the prediction of
725 appropriate end-member signatures for tracer-based hydrograph separation being valid at
726 longer time scales.

727

728 **6 Data availability**

729 Hydrometeorological data are available upon request at the Hydrographic Office of the
730 Autonomous Province of Bozen-Bolzano. Tracer data used in this study are freely available
731 by contacting the authors.

732

733 **7 Acknowledgements**

734 This research is part of the GLACIALRUN project and funded by the foundation of the Free
735 University of Bozen-Bolzano and supported by the project "Parco Tecnologico - Tecnologie
736 ambientali".

737 The authors thank Andrea Ruecker, Ana Lucia, Alex Boninsegna, Raffael Foffa, and Michiel
738 Blok for their field assistance. Giulia Zuecco and Luisa Pianezzola are thanked for the

739 isotopic analysis at TESAF, University of Padova and Christian Ceccon for the isotopic
740 analysis in the laboratory of the Free University of Bozen-Bolzano. We also thank Giulio
741 Voto at EcoResearch s.r.l. (Bozen/Bolzano) for the element analysis. We appreciate the
742 helpful support for the geological interpretation by Volkmar Mair. We acknowledged the
743 project AQUASED, whose instrumentation infrastructure we could use. Furthermore, we
744 thank the Hydrographic Office and the Department of Hydraulic Engineering of the
745 Autonomous Province of Bozen-Bolzano for providing meteorological and hydrometric data.
746 We acknowledge the Forestry Commission Office Prat, the National Park Stilfser Joch / Passo
747 Stelvio, and the Cable car Sulden GmbH for their logistical support and helpful advices.
748

749 **8 References**

- 750 Anderson, S.P., Drever, J.I., and Humphrey, N.F.: Chemical weathering in glacial
751 environments, *Geology*, 25, 399–402, 1997.
- 752 Andreatta, C.: Polymetamorphose und Tektonik in der Ortlergruppe. - *N. Jb. Mineral. Mh.*
753 *Stuttgart*, 1, 13–28, 1952.
- 754 Anslow, F. S., Hostetler, S., Bidlake, W. R. and Clark, P. U.: Distributed energy balance
755 modeling of South Cascade Glacier, Washington and assessment of model uncertainty,
756 *J. Geophys. Res.*, 113(F02019), 1–18, doi:10.1029/2007JF000850, 2008.
- 757 Auer, A. H.: The rain versus snow threshold temperatures, *Weatherwise*, 27, 67, 1974.
- 758 Baraer, M., McKenzie, J., Mark, B. G., Gordon, R., Bury, J., Condom, T., Gomez, J., Knox,
759 S. and Fortner, S. K.: Contribution of groundwater to the outflow from ungauged
760 glacierized catchments: a multi-site study in the tropical Cordillera Blanca, Peru,
761 *Hydrol. Process.*, 29, 2561–2581, doi: 10.1002/hyp.10386, 2015.
- 762 Beniston, M.: Climatic change in mountain regions: a review of possible impacts; *Clim.*
763 *Change*. 59, 5–31, doi: 10.1023/A: 1024458411589, 2003.
- 764 Beniston, M.: Mountain weather and climate: A general overview and a focus on climatic
765 change in the Alps; *Hydrobiologia*, 562, 3–16, doi: 10.1007/s10750-005-1802-0, 2006.
- 766 Beniston, M., and Stoffel, M.: Assessing the impacts of climatic change on mountain water
767 resources, *Sci. Total Environ.* 493, 1129–37, doi: 10.1016/j.scitotenv.2013.11.122,
768 2014.
- 769 Boeckli, L., Brenning, A., Gruber, S., and Noetzli, J.: A statistical approach to modelling
770 permafrost distribution in the European Alps or similar mountain ranges, *Cryosph.*, 6,
771 125–140, doi: 10.5194/tc-6-125-2012, 2012.
- 772 Braithwaite, R. J.: On glacier energy balance, ablation, and air temperature, *J. Glaciol.*, 27,
773 381–391, 1981.
- 774 Brown, G. H.: Glacier meltwater hydrochemistry, *Appl. Geochemistry*, 17(7), 855–883,
775 doi:10.1016/S0883-2927(01)00123-8, 2002.

- 776 Brown, G.H., and Fuge, R.: Trace element chemistry of glacial meltwaters in an Alpine
777 headwater catchment, *Hydrol. Water Resour. Ecol. Headwaters*, 2, 435–442, 1998.
- 778 Brown, G. H., Tranter, M., and Sharp, M.: Subglacial chemical erosion—seasonal variations
779 in solute provenance, Haut Glacier d'Arolla, Switzerland, *Ann. Glaciol.*, 22, 25-31,
780 1996.
- 781 Brown, L.E., Hannah, D.M., Milner, A.M., Soulsby, C., Hodson, A.J., and Brewer, M.J.:
782 Water source dynamics in a glacierized alpine river basin (Taillon-Gabiétous, French
783 Pyrénées), *Water Resour. Res.*, 42, doi: 10.1029/2005WR004268, 2006.
- 784 Carey, S. K., Boucher, J. L. and Duarte, C. M.: Inferring groundwater contributions and
785 pathways to streamflow during snowmelt over multiple years in a discontinuous
786 permafrost subarctic environment (Yukon, Canada), *Hydrogeol. J.*, 21, 67–77, doi:
787 10.1007/s10040-012-0920-9, 2013.
- 788 Carey, S.K. and Quinton, W.L.: Evaluating runoff generation during summer using
789 hydrometric, stable isotope and hydrochemical methods in a discontinuous permafrost
790 alpine catchment, *Hydrol. Process.*, 19, 95–114. doi:10.1002/hyp.5764, 2005. Carrillo,
791 G., Troch, P.A., Sivapalan, M., Wagener, T., Harman, C., Sawicz, K.: Catchment
792 classification: hydrological analysis of catchment behavior through process-based
793 modeling along a climate gradient, *Hydrol. Earth Syst. Sci.*, 15, 3411–3430,
794 doi:10.5194/hess-15-3411-2011, 2011.
- 795 Carturan, L., Zuecco, G., Seppi, R., Zanoner, T., Borga, M., Carton, A. and Dalla Fontana, G.:
796 Catchment-Scale Permafrost Mapping using Spring Water Characteristics, *Permafr.*
797 *Periglac. Process.*, 27(3), 253–270, doi:10.1002/ppp.1875, 2016.
- 798
- 799 Chiogna, G., Majone, B., Cano Paoli, K., Diamantini, E., Stella, E., Mallucci, S., Lencioni,
800 V., Zandonai, F. and Bellin, A.: A review of hydrological and chemical stressors in the
801 adige catchment and its ecological status, *Sci. Total Environ.* 540, 429–443,
802 doi:10.1016/j.scitotenv.2015.06.149, 2016.
- 803 Clark, I.D., Lauriol, B., Harwood, L., Marschner, M.: Groundwater contributions to discharge
804 in a permafrost setting, Big Fish River, N.W.T., Canada, *Arct. Antarct. Alp. Res.*, 33,

805 62–69, 2001.

806 Coléou, C., and Lesaffre, B.: Irreducible water saturation in snow: experimental results in a
807 cold laboratory, *Ann. Glaciol.*, 26, 64–68, 1998.

808 Colombo, N., Salerno, F., Gruber, S., Freppaz, M., Williams, M., Fratianni, S. and Giardino,
809 M.: Review: Impacts of permafrost degradation on inorganic chemistry of surface
810 fresh water, *Glob. Planet. Change*, 162, 69–83, doi:10.1016/j.gloplacha.2017.11.017,
811 2017.

812 Cook, S.J., and Swift, D.A.: Subglacial basins: Their origin and importance in glacial systems
813 and landscapes, *Earth-Science Rev.* 115, 332–372, doi:
814 10.1016/j.earscirev.2012.09.009, 2012.

815 Cortés, G., Vargas, X., McPhee, J.: Climatic sensitivity of streamflow timing in the
816 extratropical western Andes Cordillera, *J. Hydrol.*, 405, 93–109, doi:
817 10.1016/j.jhydrol.2011.05.013, 2011.

818 Devito, K., Creed, I., Gan, T., Mendoza, C., Petrone, R., Silins, U., and Smerdon, B.: A
819 framework for broad-scale classification of hydrologic response units on the Boreal
820 Plain: Is topography the last thing to consider? *Hydrol. Process.*, 19, 1705–1714,
821 doi:10.1002/hyp.5881, 2005.

822 Dye, D.G.: Variability and trends in the annual snow-cover cycle in Northern Hemisphere
823 land areas, 1972-2000, *Hydrol. Process.*, 16, 3065–3077, doi:10.1002/hyp.1089, 2002.

824 Engel, M., Penna, D., Bertoldi, G., Dell’Agnese, A., Soulsby, C., and Comiti, F.: Identifying
825 run-off contributions during melt-induced runoff events in a glacierized Alpine
826 catchment, *Hydrol. Process.*, 30, 343–364, doi:10.1002/hyp.10577, 2016.

827 Engel, M., Penna, D., Tirlir, W., and Comiti F.: Multi-Parameter-Analyse zur
828 Charakterisierung von Landschaftsmerkmalen innerhalb eines experimentellen
829 Messnetzes im Hochgebirge, In M. Casper et al. (Eds.): *Den Wandel Messen –*
830 *Proceedings Tag der Hydrologie 2017, Forum für Hydrologie und*
831 *Wasserbewirtschaftung*, Vol. 38, 293 – 299, 2017.

- 832 Engel, M., Brighenti S., Bruno MC., Tolotti M., Comiti F.: Multi-tracer approach for
833 characterizing rock glacier outflow, 5th European Conference on Permafrost,
834 Chamonix-Mont Blanc, 2018.
- 835 Epstein, S. and Mayeda, T.: Variation of $\delta^{18}\text{O}$ content in waters from natural sources,
836 *Geochim. Cosmochim. Ac.*, 4, 213–224, 1953.
- 837 Farvolden, R.N., Geological controls on ground-water storage and base flow, *J. Hydrol.*, 1,
838 219–249, 1963.
- 839 Freyberg, J. Von, Studer, B. and Kirchner, J. W.: A lab in the field : high-frequency analysis
840 of water quality and stable isotopes in stream water and precipitation, *Hydrol. Earth*
841 *Syst. Sci.*, 21, 1721–1739, doi:10.5194/hess-21-1721-2017, 2017.
- 842 Fischer, B. M. C., Rinderer, M., Schneider, P., Ewen, T. and Seibert, J.: Contributing sources
843 to baseflow in pre-alpine headwaters using spatial snapshot sampling, *Hydrol.*
844 *Process.*, 29, 5321–5336, doi:10.1002/hyp.10529, 2015.
- 845 Gabrielli, P., Cozzi, G., Torcini, S., Cescon, P., Barbante, C.: Source and origin of
846 atmospheric trace elements entrapped in winter snow of the Italian Eastern Alps,
847 *Atmos. Chem. Phys. Discuss.*, 6, 8781–8815, doi: 10.5194/acpd-6-8781-2006, 2006.
- 848 Galos, S.P., Klug, C., Prinz, R., Rieg, L., Sailer, R., Dinale, R., Kaser, G.: Recent glacier
849 changes and related contribution potential to river discharge in the Vinschgau / Val
850 Venosta, Italian Alps, *Geogr. Fis. e Din. Quat.*, 38, 143–154,
851 doi:10.4461/GFDQ.2015.38.13, 2015.
- 852 Gat, J. R. and Carmi, I.: Evolution of the isotopic composition of atmospheric waters in the
853 Mediterranean Sea area, *J. Geophys. Res.*, 75, 3039–3048, 1970.
- 854 Genereux, D.: Quantifying uncertainty in tracer-based hydrograph separations, *Water Resour.*
855 *Res.*, 34, 915–919, 1998.
- 856 Gordon, R. P., Lautz, L. K., McKenzie, J. M., Mark, B. G., Chavez, D. and Baraer, M.:
857 Sources and pathways of stream generation in tropical proglacial valleys of the
858 Cordillera Blanca, Peru, *J. Hydrol.*, 522, 628–644, doi: 10.1016/j.jhydrol.2015.01.013
859 2015.

- 860 Gruber, S., Fleiner, R., Guegan, E., Panday, P., Schmid, M.O., Stumm, D., Wester, P., Zhang,
861 Y., and Zhao, L.: Review article: Inferring permafrost and permafrost thaw in the
862 mountains of the Hindu Kush Himalaya region, *Cryosph.*, 11, 81–99, doi:10.5194/tc-
863 11-81-2017, 2017.
- 864 Guo, B., Liu, Y., Zhang, F., Hou, J. and Zhang, H.: Heavy metals in the surface sediments of
865 lakes on the Tibetan Plateau, China, *Environ. Sci. Pollut. Res.*, 25(4), 3695–3707, doi:
866 10.1007/s11356-017-0680-0, 2017.
- 867 Harris, C., Haeberli, W., Mühlh, D.Vonder, and King, L.: Permafrost monitoring in the high
868 mountains of Europe: the PACE project in its global context, *Permafr. Periglac.*
869 *Process.*, 12, 3–11, doi:10.1002/ppp, 2001.
- 870 Heidbüchel, I., Troch, P. A. and Lyon, S. W.: Separating physical and meteorological controls
871 of variable transit times in zero-order catchments, *Water Resour. Res.*, 49(11), 7644–
872 7657, doi:10.1002/2012WR013149, 2013.
- 873 Hindshaw, R.S., Tipper, E.T., Reynolds, B.C., Lemarchand, E., Wiederhold, J.G.,
874 Magnusson, J., Bernasconi, S.M., Kretzschmar, R., and Bourdon, B.: Hydrological
875 control of stream water chemistry in a glacial catchment (Damma Glacier,
876 Switzerland), *Chem. Geol.*, 285, 215–230, doi:10.1016/j.chemgeo.2011.04.012, 2011.
- 877 Hock, R.: A distributed temperature-index ice- and snowmelt model including potential direct
878 solar radiation, *J. Glaciol.*, 45, 101–11, 1999.
- 879 Hodgkins, R.: Seasonal evolution of meltwater generation, storage and discharge at a non-
880 temperate glacier in Svalbard, *Hydrol. Process.*, 15, 441–460, 10.1002/hyp.160, 2001.
- 881 Humlum, O.: The geomorphic significance of rock glaciers: estimates of rock glacier
882 debris volumes and headwall recession rates in West Greenland, *Geomorphology*, 35,
883 41–67, 2000.
- 884 International Atomic Energy Agency: IAEA/GNIP precipitation sampling guide V2.02
885 September 2014, International Atomic Energy Agency, Vienna, Austria, pp. 19, 2014.
- 886 IPCC, 2013. Climate Change 2013: The Physical Science Basis. Contribution of Working
887 Group I to the Fifth Assessment Report of the Intergovernmental Panel on Climate
888 Change. In: Stocker, T.F., Qin, D., Plattner, G.-K., Tignor, M., Allen, S.K., Boschung,
889 J., Nauels, A., Xia, Y., Bex, V., Midgley, P.M., (Eds.), International Organization for

890 Standardization Standard Atmosphere, ISO 2533, Cambridge University Press,
891 Cambridge, United Kingdom and New York, NY, USA, 1535, pp. ISO, 1975.

892 Kaser, G., Grosshauser, M., and Marzeion, B.: Contribution potential of glaciers to water
893 availability in different climate regimes, in: Proceedings of the National Academy of
894 Sciences of the United States of America, 20223–20227,
895 doi:10.1073/pnas.1008162107, 2010.

896 Katsuyama, M., Tani, M., and Nishimoto S.: Connection between streamwater mean
897 residence time and bedrock groundwater recharge/discharge dynamics in weathered
898 granite catchments, *Hydrol. Process.*, 24, 2287–2299, doi:10.1002/hyp.7741, 2010.

899 Kirchner, J.W.: Catchments as simple dynamical systems: Catchment characterization,
900 rainfall-runoff modeling, and doing hydrology backward, *Water Resour. Res.*, 45,
901 W02429, doi:10.1029/2008WR006912, 2009.

902 Kong, Y., and Pang, Z.: Evaluating the sensitivity of glacier rivers to climate change based on
903 hydrograph separation of discharge, *J. Hydrol.* 434–435, 121–129,
904 doi:10.1016/j.jhydrol.2012.02.029, 2012.

905 Krainer, K., and Mostler, W.: Hydrology of active rock glaciers: examples from the Austrian
906 Alps, *Arct. Antarct. Alp. Res.*, 34, 142–149, 2002.

907 Krainer, K., Mostler, W., and Spötl, C.: Discharge from active rock glaciers, Austrian Alps: a
908 stable isotope approach, *Austrian J. Earth Sc.*, 100, 102–112, 2007.

909 Krainer, K., Bressan, D., Dietre, B., Haas, J.N., Hajdas, I., Lang, K., Mair, V., Nickus, U.,
910 Reidl, D., Thies, H., and Tonidandel, D.: A 10,300-year-old permafrost core from the
911 active rock glacier Lazaun, southern Ötztal Alps (South Tyrol, northern Italy), *Quat.*
912 *Res.*, 83, 324–335, doi:10.1016/j.yqres.2014.12.005, 2015.

913 Lamhonwah, D., Lafrenière, M.J., Lamoureux, S.F., and Wolfe, B.B.: Evaluating the
914 hydrological and hydrochemical responses of a High Arctic catchment during an
915 exceptionally warm summer, *Hydrol. Process.*, 31, 2296–2313, doi:
916 10.1002/hyp.11191, 2017.

917 Lewis, T., Lafrenière, M.J., and Lamoureux, S.F.: Hydrochemical and sedimentary responses
918 of paired High Arctic watersheds to unusual climate and permafrost disturbance, Cape

- 919 Bounty, Melville Island, Canada, *Hydrol. Process.*, 26, 2003–2018,
920 doi:10.1002/hyp.8335, 2012.
- 921 Liu, F., Williams, M.W., and Caine, N.: Source waters and flow paths in an alpine catchment,
922 Colorado Front Range, United States, *Water Resour. Res.*, 40,
923 doi:10.1029/2004WR003076, 2004.
- 924 Mair, V.: Die Kupferbergbaue von Stilfs, Eysrs und Klausen, *Der Stoansucher* 10 (1), 38–44,
925 1996.
- 926 Mair, V., Lorenz, D., and Eschgfäller, M.: *Mineralienwelt Südtirol*. Verlag Tappeiner, Lana
927 (BZ), 215 S., 2009.
- 928 Mair, V., Müller, J.P., and Reisigl, H.: *Leben an der Grenze*. Konsortium Nationalpark
929 Stilfserjoch – Gemeinde Stilfs, Glurns (BZ), 120 S., 2002.
- 930 Mair, V., Nocker, C., and Tropper, P.: Das Ortler-Campo Kristallin in Südtirol, *Mitt. Österr.*
931 *Mineral. Ges.*, 153, 219–240, 2007.
- 932 Mair, V., Zischg, A., Lang, K., Tonidandel, D., Krainer, K., Kellerer-Pirklbauer, A., Deline,
933 P., Schoeneich, P., Cremonese, E., Pogliotti, P., Gruber, S. and Böckli, L.: PermaNET
934 - Permafrost Long-term Monitoring Network. Synthesis report. INTERPRAEVENT
935 Journal series 1, Report 3. Klagenfurt, 2011.
- 936 Maurya, A.S., Shah, M., Deshpande, R.D., Bhardwaj, R.M., Prasad, A., and Gupta, S.K.:
937 Hydrograph separation and precipitation source identification using stable water
938 isotopes and conductivity: River Ganga at Himalayan foothills, *Hydrol. Process.*, 25,
939 1521–1530, doi:10.1002/hyp.7912, 2011.
- 940 McClymont, A.F., Hayashi, M., Bentley, L.R., Muir, D., and Ernst, E.: Groundwater flow
941 and storage within an alpine meadow-talus complex, *Hydrol. Earth Syst. Sci.*, 14, 859–
942 872, doi:10.5194/hess-14-859-2010, 2010.
- 943 McGuire, K. J., McDonnell, J. J., Weiler, M., Kendall, C., McGlynn, B. L., Welker, J. M., and
944 Seibert, J.: The role of topography on catchment-scale water residence time. *Water*
945 *Resour. Res.*, 41. doi:10.1029/2004WR003657, 2005.

- 946 Milly, P.C.D., Betancourt, J., Falkenmark, M., Hirsch, R.M., Kundzewicz, Z.W., Lettenmaier,
947 D.P., Stouffer, R.J.: Stationarity is dead—whither water management? *Science*, 319,
948 573–574, doi:10.1126/science.1151915, 2008.
- 949 Milner, A., Brown, L.E., and Hannah, D.M.: Hydroecological response of river systems to
950 shrinking glaciers, *Hydrol. Process.* 23, 62–77, doi:10.1002/hyp.7197 2009.
- 951 Montrasio, A. Berra, F., Cariboni, M., Ceriani, M., Deichmann, N., Ferliga, C., Gregnanin,
952 A., Guerra, S., Guglielmin, M., Jadoul, F., Lonhghin, M., Mair, V., Mazzoccola, D.,
953 Sciesa, E. & Zappone, A.: Note illustrative della Carta geologica d'Italia alla scala
954 1:50.000 Foglio 024 Bormio. ISPRA, Servizio Geologico D'Italia; System Cart, Roma
955 2012, 150 S., 2012.
- 956 Moore, R. D., Fleming, S. W., Menounos, B., Wheate, R., Fountain, A., Stahl, K., Holm, K.
957 and Jakob, M.: Glacier change in western North America: influences on hydrology,
958 geomorphic hazards and water quality, *Hydrol. Process.*, 23, 42–61,
959 10.1002/hyp.7162, 2009.
- 960 Mutzner, R., Weijs, S. V., Tarolli, P., Calaf, M., Oldroyd, J., and Parlange, M.B.: Controls on
961 the diurnal streamflow cycles in two subbasins of an alpine headwater catchment,
962 *Water Resour. Res.*, 51, 3403–3418, doi:10.1016/0022-1694(68)90080-2, 2015.
- 963 Natali, C., Bianchini, G., Marchina, C., and Knöller, K.: Geochemistry of the Adige River
964 water from the Eastern Alps to the Adriatic sea (Italy): Evidences for distinct
965 hydrological components and water-rock interactions. *Environ. Sci. Pollut. R.*, 23,
966 11677-11694. doi:10.1007/s11356-016-6356-3, 2016.
- 967 Nickus U., Krainer K., Thies H. and Tolotti M.: Blockgletscherabflüsse am Äußeren
968 Hochebenkar –Hydrologie, Wasserchemie und Kieselalgen. In: Schallart N. &
969 Erschbamer B. (eds), *Forschung am Blockgletscher, Methoden und Ergebnisse*. Alpine
970 Forschungstelle Obergurgl, Innsbruck University Press, Innsbruck (A), 4: 117-134.
971 ISBN 978-3-902936-58-5, 2015.
- 972 Nordstrom, D. K. Hydrogeochemical processes governing the origin, transport and fate of
973 major and trace elements from mine wastes and mineralized rock to surface waters,
974 *Appl. Geochem.*, 26, 1777–1791, 2011.

- 975 Onda, Y., Komatsu, Y., Tsujimura, M., and Fujihara, J. I.: The role of subsurface runoff
976 through bedrock on storm flow generation, *Hydrol. Processes*, 15, 1693–1706,
977 doi:10.1002/hyp.234, 2001.
- 978 Penna, D., Stenni, B., Šanda, M., Wrede, S., Bogaard, T.A., Gobbi, A., Borga, M., Fischer,
979 B.M.C., Bonazza, M., and Chárová, Z.: On the reproducibility and repeatability of
980 laser absorption spectroscopy measurements for $\delta^2\text{H}$ and $\delta^{18}\text{O}$ isotopic analysis,
981 *Hydrol. Earth Syst. Sci.*, 14, 1551–1566, doi:10.5194/hess-14-1551-2010, 2010.
- 982 Penna, D., Stenni, B., Šanda, M., Wrede, S., Bogaard, T.A., Michelini, M., Fischer, B.M.C.,
983 Gobbi, A., Mantese, N., Zuecco, G., Borga, M., Bonazza, M., Sobotková, M.,
984 Čejková, B. and Wassenaar, L.I.: Technical Note: Evaluation of between-sample
985 memory effects in the analysis of $\delta^2\text{H}$ and $\delta^{18}\text{O}$ of water samples measured by laser
986 spectrometers, *Hydrol. Earth Syst. Sci.*, 16, 3925–3933, doi:10.5194/hess-16-3925-
987 2012, 2012.
- 988 Penna, D., Engel, M., Mao, L., Agnese, A. D., Bertoldi, G. and Comiti, F.: Tracer-based
989 analysis of spatial and temporal variations of water sources in a glacierized catchment,
990 *Hydrol. Earth Syst. Sci.*, 18, 5271–5288, 10.5194/hess-18-5271-2014, 2014.
- 991 Penna, D., Engel, M., Bertoldi, G., and Comiti, F.: Towards a tracer-based conceptualization
992 of meltwater dynamics and streamflow response in a glacierized catchment, *Hydrol.*
993 *Earth Syst. Sci.*, 21, 23–41, 10.5194/hess-21-23-2017, 2017.
- 994 Peralta-Tapia, A., Sponseller, R. A., Ågren, A., Tetzlaff, D., Soulsby, C., and Laudon, H.:
995 Scale-dependent groundwater contributions influence patterns of winter baseflow
996 stream chemistry in boreal catchments, *J. Geophys. Res. Biogeo.*, 120, 847–858.
997 doi:10.1002/2014JG002878, 2015.
- 998 R Core Team: *R: A Language and Environment for Statistical Computing*. R Foundation for
999 Statistical Computing, Vienna, Austria, 2016.
- 1000 Ragettli, S., Immerzeel, W.W., and Pellicciotti, F.: Contrasting climate change impact on
1001 river flows from high-altitude catchments in the Himalayan and Andes Mountains,
1002 *Proc. Natl. Acad. Sci.*, 113, 9222–9227, doi:10.1073/pnas.1606526113, 2016.

- 1003 Ragetti, S., and Pellicciotti, F.: Calibration of a physically based, spatially distributed
1004 hydrological model in a glacierized basin: On the use of knowledge from
1005 glaciometeorological processes to constrain model parameters, *Water Resour. Res.*,
1006 48, 1–20, doi:10.1029/2011WR010559, 2012.
- 1007 Rinaldo, A., Benettin, P., Harman, C.J., Hrachowitz, M., Mcguire, K.J., Velde, Y. Van Der,
1008 Bertuzzo, E., Botter, G.: Storage selection functions: A coherent framework for
1009 quantifying how catchments store and release water and solutes, *Water Resources Res.*
1010 51, doi:10.1002/2015WR017273, 2015.
- 1011 Rogger, M., Chirico, G.B., Hausmann, H., Krainer, K., Brückl, E., Stadler, P., Blöschl, G.:
1012 Impact of mountain permafrost on flow path and runoff response in a high alpine
1013 catchment, *Water Resour. Res.*, 53 (2), 1288–1308, 2017.
- 1014 Roy, J.W., and Hayashi, M.: Multiple, distinct groundwater flow systems of a single moraine–
1015 talus feature in an alpine watershed, *J. Hydrol.*, 373, 139–150, doi:
1016 10.1016/j.jhydrol.2009.04.018, 2009.
- 1017 Rutter, N., Hodson, A., Irvine-Fynn, T., and Solås, M.K.: Hydrology and hydrochemistry of a
1018 deglaciating high-Arctic catchment, Svalbard, *J. Hydrol.* 410, 39–50,
1019 doi:10.1016/j.jhydrol.2011.09.001, 2011.
- 1020 Schaefli, B., Maraun, D. and Holschneider, M.: What drives high flow events in the Swiss
1021 Alps? Recent developments in wavelet spectral analysis and their application to
1022 hydrology, *Adv. Water Resour.*, 30, 2511–2525, doi:10.1016/j.advwatres.2007.06.004,
1023 2007.
- 1024 Schmieder, J., Marke, T., and Strasser, U. Tracerhydrologische Untersuchungen im Rofental
1025 (Öztaler Alpen / Österreich). *Innsbrucker Jahresbericht, Institut für Geographie der*
1026 *Universität Innsbruck*, 109 – 120, 2017.
- 1027 Schwarb, M.: *The Alpine Precipitation Climate*. Swiss Federal Institut of Technology Zurich,
1028 2000.
- 1029 Shevchenko, V. P., Pokrovsky, O. S., Vorobyev, S. N., Krickov, I. V., Manasypov, R. M.,
1030 Politova, N. V., Kopysov, S. G., Dara, O. M., Auda, Y., Shirokova, L. S.,
1031 Kolesnichenko, L. G., et al.: Impact of snow deposition on major and trace element

- 1032 concentrations and fluxes in surface waters of Western Siberian Lowland, *Hydrol.*
1033 *Earth Syst. Sci.*, 21, 5725–5746, doi:10.5194/hess-2016-578, 2016.
- 1034 Sicart, J.E., Pomeroy, J.W., Essery, R.L.H., Bewley, D.: Incoming longwave radiation to
1035 melting snow: Observations, sensitivity and estimation in northern environments.
1036 *Hydrol. Process.* 20, 3697–3708, doi:10.1002/hyp.6383, 2006.
- 1037 Sicart, J. E., Hock, R. and Six, D.: Glacier melt, air temperature, and energy balance in
1038 different climates: The Bolivian Tropics, the French Alps, and northern Sweden, *J.*
1039 *Geophys. Res.*, 113, 1–11, doi: 10.1029/2008JD010406, 2008.
- 1040 Singh, P., Haritashya, U.K., Ramasastri, K.S., and Kumar, N.: Diurnal variations in discharge
1041 and suspended sediment concentration, including runoff-delaying characteristics, of
1042 the Gangotri Glacier in the Garhwal Himalayas, *Hydrol. Process.*, 19, 1445–1457,
1043 doi:10.1002/hyp.5583, 2005.
- 1044 Sivapalan, M.: Prediction in ungauged basins: a grand challenge for theoretical hydrology,
1045 *Hydrol. Process.* 17, 3163–3170, doi:10.1002/hyp.5155, 2003
- 1046 Sklash, M. G., R. N. Farvolden, and Fritz, P.: A conceptual model of watershed response to
1047 rainfall, developed through the use of oxygen-18 as a natural tracer, *Can. J. Earth Sci.*,
1048 13, 271-283, 1976.
- 1049 Soulsby, C., Tetzlaff, D., Dunn, S. M. and Waldron, S.: Scaling up and out in runoff process
1050 understanding: Insights from nested experimental catchment studies, *Hydrol. Process.*,
1051 20, 2461–2465, doi: 10.1002/hyp.6338, 2006a.
- 1052 Soulsby, C., Tetzlaff, D., Rodgers, P., Dunn, S. and Waldron, S.: Runoff processes, stream
1053 water residence times and controlling landscape characteristics in a mesoscale
1054 catchment: An initial evaluation, *J. Hydrol.*, 325, 197–221, doi:
1055 10.1016/j.jhydrol.2005.10.024, 2006b.
- 1056 Sprenger, M., Leistert, H., Gimbel, K. and Weiler, M.: Illuminating hydrological processes at
1057 the soil-vegetation-atmosphere interface with water stable isotopes, *Rev. Geophys.*,
1058 54, 674–704, doi:10.1002/2015RG000515, 2016.
- 1059 Staudinger, M., Stoelzle, M., Seeger, S., Seibert, J., Weiler, M. and Stahl K.: Catchment water
1060 storage variation with elevation, *Hydrol. Process.*, 31, 2000–2015, doi:

- 1061 10.1002/hyp.11158, 2017.
- 1062 Stingl, V. and Mair, V.: An introduction to the geology of South Tyrol. Autonome Provinz
1063 Bozen, Amt für Geologie und Baustoffprüfung, Kardaun (BZ), 80 S., 2005.
- 1064 Swift, D. A., Nienow, P. W., Hoey, T. B. and Mair, D. W. F.: Seasonal evolution of runoff
1065 from Haut Glacier d’Arolla, Switzerland and implications for glacial geomorphic
1066 processes, *J. Hydrol.*, 309, 133–148, doi:10.1016/j.jhydrol.2004.11.016, 2005.
- 1067 Taylor, S., Feng, X., Kirchner, J.W., Osterhuber, R., Klaue, B. and Renshaw, C.E.: Isotopic
1068 evolution of a seasonal snowpack and its melt, *Water Resour. Res.* 37: 759–769.
1069 DOI:10.1029/2000WR900341, 2001.
- 1070 Tetzlaff, D., Seibert, J., McGuire, K. J., Laudon, H., Burns, D. A., Dunn, S. M. and Soulsby,
1071 C.: How does landscape structure influence catchment transit time across different
1072 geomorphic provinces, *Hydrol. Process.*, 23, 945–953, 2009.
- 1073 Tetzlaff, D., Buttle, J., Carey, S.K., McGuire, K., Laudon, H., and Soulsby, C.: Tracer-based
1074 assessment of flow paths, storage and runoff generation in northern catchments: a
1075 review, *Hydrol. Process.*, 29, 3475–3490, doi: 10.1002/hyp.10412, 2014.
- 1076 Thies, H., Nickus, U., Mair, V., Tessadri, R., Tait, D., Thaler, B. and Psenner, R.: Unexpected
1077 response of high Alpine Lake waters to climate warming, *Environ. Sci. Technol.*, 41,
1078 7424–9, 2007.
- 1079 Thies, H., Nickus, U., Tolotti, M., Tessadri, R., Krainer, K., Evidence of rock glacier melt
1080 impacts on water chemistry and diatoms in high mountain streams, *Cold Reg. Sci.*
1081 *Technol.*, 96, 77–85, doi:10.1016/j.coldregions.2013.06.006, 2013.
- 1082 Uhlenbrook, S. and Hoeg, S.: Quantifying uncertainties in tracer-based hydrograph
1083 separations : a case study for two- , three- and five-component hydrograph separations
1084 in a mountainous catchment, *Hydrol. Process.*, 17, 431–453, doi:10.1002/hyp.1134,
1085 2003.
- 1086 U.S. Army Corps of Engineers: Summary Report of the Snow Investigations, Snow
1087 Hydrology , North Pacific Division, Portland, Oregon, 1956.

- 1088 Vaughn, B. H. and Fountain, A. G.: Stable isotopes and electrical conductivity as keys to
1089 understanding water pathways and storage in South Cascade Glacier, Washington,
1090 USA, *Ann. Glaciol.*, 40, 107–112, doi: 10.3189/172756405781813834, 2005.
- 1091 Vincent, C. and Six, D.: Relative contribution of solar radiation and temperature in enhanced
1092 temperature-index melt models from a case study at Glacier de Saint-Sorlin, France,
1093 *Ann. Glaciol.*, 54(63), 11–17, doi:10.3189/2013AoG63A301, 2013.
- 1094 Viviroli, D., Archer, D.R., Buytaert, W., Fowler, H.J., Greenwood, G.B., Hamlet, A. F.,
1095 Huang, Y., Koboltschnig, G.R., Litaor, M.I., López-Moreno, J.I., Lorentz, S.,
1096 Schädler, B., Schreier, H., Schwaiger, K., Vuille, M., and Woods, R.: Climate change
1097 and mountain water resources: overview and recommendations for research,
1098 management and policy, *Hydrol. Earth Syst. Sci.*, 15, 471–504, doi:10.5194/hess-15-
1099 471-2011, 2011.
- 1100 Weiler, M., Seibert, J. and Stahl, K.: Magic components - why quantifying rain, snow- and
1101 icemelt in river discharge isn't easy, *Hydrol. Process.*, doi:10.1002/hyp.11361, 2017.
- 1102 Williams, M.W., Knauf, M., Caine, N., Liu, F., Verplanck, P.L.: Geochemistry and source
1103 waters of rock glacier outflow, Colorado Front Range, *Permafr. Periglac. Process.*, 17,
1104 13–33, doi:10.1002/ppp.535, 2006.
- 1105 Williams, M.W., Hood, E., Molotch, N.P., Caine, N., Cowie, R., and Liu, F.: The 'teflon
1106 basin' myth: hydrology and hydrochemistry of a seasonally snow-covered catchment,
1107 *Plant Ecol. Divers.*, 8, 639-661, doi:10.1080/17550874.2015.1123318,2015.
- 1108 Wolfe, P.M. and English, M.C.: Hydrometeorological relationships in a glacierized catchment
1109 in the Canadian high Arctic, *Hydrol. Process.*, 9, 911–921, doi:
1110 10.1002/hyp.3360090807, 1995.
- 1111 Wolock, D. M., Fan, J., and Lawrence, G. B.: Effects of basin size on low-flow stream
1112 chemistry and subsurface contact time in the Neversink River watershed, New York,
1113 *Hydrol. Process.*, 11, 1273-1286, 1997.
- 1114 Wu, X.: Diurnal and seasonal variation of glacier meltwater hydrochemistry in Qiyi
1115 glacierized catchment in Qilian mountains, northwest china: Implication for chemical
1116 weathering, *J. Mt. Sci.*, 15, 1035-1045, doi:10.1007/s11629-017-4695-2, 2018.

- 1117 Xing, B., Liu, Z., Liu, G., Zhang, J.: Determination of runoff components using path analysis
1118 and isotopic measurements in a glacier-covered alpine catchment (upper Hailuogou
1119 Valley) in southwest China, *Hydrol. Process.*, 29, 3065–3073, doi:10.1002/hyp.10418,
1120 2015.
- 1121 Zhou, S., Wang, Z. and Joswiak, D. R.: From precipitation to runoff: stable isotopic
1122 fractionation effect of glacier melting on a catchment scale, *Hydrol. Process.*, 28,
1123 3341–3349, doi: 10.1002/hyp.9911, 2014.
- 1124 Zuecco, G., Penna, D., Borga, M., and van Meerveld, H. J.: A versatile index to characterize
1125 hysteresis between hydrological variables at the runoff event timescale, *Hydrol.*
1126 *Process*, 30, 1449–1466. doi:10.1002/hyp.10681, 2016.
- 1127 Zuzel, J.F., and Cox, L.M.: Relative importance of meteorological variables in snowmelt,
1128 *Water Resour. Res.*, 11, 174–176, 1975.
- 1129

1130 Table 1. Meteorological characteristics of the weather station Madritsch/Madriccio 2.825 m
1131 a.s.l. in 2014 and 2015.

Date	2014	2015
Precipitation (total / rain / snow) (mm y ⁻¹)*	1284/704/579	961/637/323
Mean annual air temperature (°C)	-1.4	-0.8
Days with snow cover > 10cm	270	222
Maximum snow depth (date)	02/03/2014	27/03/2015
Maximum snow depth (cm)	253	118
Date of snow cover disappearance	12/07/2014	13/06/2015
Median discharge (m ³ s ⁻¹)	9.5	5.2

1132 * Precipitation data are not wind-corrected. Rain vs. snow separation was performed
1133 following Auer (1974)
1134

1135 Table 2. Topographical characteristics of sub-catchments defined by sampling points.

Sampling point	Description	Catchment area (km ²)	Glacier cover (%)	Elevation range
T1	Trafoi River	51.28	35	1587 - 3469
T2	Trafoi River	46.72	18.6	1404 - 3889
T3	Trafoi River	12.18	17	1197 - 3889
TT1	Tributary draining Trafoi glacier	4.32	27.1	1587 - 3430
TT2	Small creek	0.05	0	1607 - 2082
TT3	Tributary draining Zirkus/ Circo glacier	6.46	44	1605 - 3888
TSPR1	Spring at the foot of a slope	-	0	1602*
TSPR2	Spring at the foot of a slope	-	0	1601*
S1	Sulden River	130.14	13.6	1109 - 3896
S2	Sulden River	74.61	12.1	1296 - 3896
S3	Sulden River	57.01	15.8	1707 - 3896
S4	Sulden River	45.06	18.6	1838 - 3896
S5	Sulden River	18.91	29.7	1904 - 3896
S6	Sulden River	14.27	38.5	2225 - 3896
ST1	Razoi tributary	6.46	0.6	1619 - 3368
ST2	Zay tributary	11.1	12.8	1866 - 3543
ST3	Rosim tributary	7.3	9.7	1900 - 3542

SSPR1	Spring in the valley bottom near Sulden town	-	0	1841*
SSPR2 - 4	At the base of the rock glacier front	-	0.12**	2614, 2594, 2600*

1136 * for spring locations, the elevation of the sampling point is given.

1137 ** for rock glacier spring locations, the glacier cover refers to the extent of both rock glaciers.

1138

1139 Table 3. Nivo-meteorological indicators derived from the weather station

1140 Madritsch/Madriccio at 2825 m a.s.l..

Variable	Unit	Description
P_{1d}	mm	Cumulated precipitation of the sampling day
P_{nd}		Cumulated precipitation n days prior to sampling day
T_{max1d}	°C	Maximum air temperature during the sampling day
T_{maxnd}		Maximum air temperature within n days prior to sampling day
G_{max1d}	W/m ²	Maximum global solar radiation during sampling day
G_{maxnd}		Maximum global solar radiation within n days prior to sampling day
ΔSD_{1d}	cm	Difference of snow depth measured at the sampling day at 12:00 and the previous day at 12:00, based on 6h averaged snow depth records.
ΔSD_{nd}		Difference of snow depth measured at the sampling day at 12:00 and n days prior the sampling day at 12:00, based on 6h averaged snow depth records.
D_{Prec1}	days	Days since last daily cumulated precipitation of > 1mm was measured.
D_{Prec10}		Days since last daily cumulated precipitation of > 10mm was measured.
D_{Prec20}		Days since last daily cumulated precipitation of > 20mm was measured.

1 Table 4. Statistics of element concentration (in $\mu\text{g l}^{-1}$) from selected stream, tributary and active rock glacier springs in the Sulden catchment
 2 sampled from March to October 2015. CV: coefficient of variation. VC: variability coefficient (see Eq. 1) with SD_{baseflow} (based on samples
 3 from March, April, and October 2015) and SD_{melting} (based on samples from May to September 2015). Note that CV was not calculated for
 4 SSPR2 – 4 as water samples were available only during summer.

Location	Statistic	Na	Mg	Al	K	Ca	V	Cr	Mn	Fe	Ni	Cu
S1	min	1881.3	12169.1	6.9	1051.2	41497.2	0.2	0.2	1.1	21.1	0.5	1.5
	max	7246.9	19547.1	541.4	2456.0	56508.3	1.8	1.4	62.4	1038.9	3.8	9.1
	mean	3253.5	14625.4	148.7	1657.3	48423.7	0.6	0.6	15.0	292.5	1.3	4.9
	SD	1782.0	2265.3	157.3	487.1	4538.1	0.5	0.3	18.7	300.2	1.0	3.0
	CV	0.5	0.2	1.1	0.3	0.1	0.9	0.5	1.2	1.0	0.8	0.6
	VC	0.6	0.3	0.3	1.6	0.5	0.2	0.2	0.1	0.3	0.2	0.8
S2	min	1968.4	9793.3	6.1	1546.3	43167.9	0.1	0.2	1.1	12.0	0.3	1.3
	max	3334.6	16453.8	743.1	2476.3	73177.3	1.9	1.7	71.0	1513.5	3.8	9.1
	mean	2431.6	12437.2	211.2	1900.9	52361.7	0.6	0.6	18.5	410.7	1.2	3.3
	SD	409.4	2292.5	236.4	299.3	8738.1	0.6	0.5	22.4	467.9	1.1	2.4

	CV	0.2	0.2	1.1	0.2	0.2	1.0	0.8	1.2	1.1	0.9	0.7
	VC	2.0	0.2	0.2	0.7	0.2	0.1	0.2	0.1	0.2	0.2	0.2
S6	min	1262.6	17458.6	9.0	1042.6	67588.1	0.1	0.1	1.5	21.6	0.5	1.5
	max	2277.0	34928.5	799.4	1748.4	166731.5	3.4	1.9	104.6	1587.1	6.2	17.0
	mean	1805.6	22862.4	278.4	1362.7	129896.0	1.1	0.8	43.1	596.1	2.1	6.5
	SD	339.4	5512.9	321.0	259.4	28165.0	1.2	0.7	47.4	670.0	1.9	4.9
	CV	0.2	0.2	1.2	0.2	0.2	1.2	0.8	1.1	1.1	0.9	0.8
	VC	0.6	0.2	0.0	1.4	0.5	0.0	0.1	0.0	0.1	0.1	0.2
SSPR2-4	min	1768.3	10051.4	9.0	1236.1	76848.5	0.0	0.1	1.5	16.7	0.2	0.5
	max	2818.6	29509.5	321.2	2402.5	131149.7	2.5	0.6	71.7	492.2	1.5	38.3
	mean	2199.9	17254.4	68.9	2009.0	94611.4	0.4	0.3	13.1	127.5	0.7	8.2
	SD	343.3	6935.8	97.8	294.4	21508.4	0.8	0.2	22.5	148.5	0.5	11.7
	CV	0.2	0.4	1.4	0.1	0.2	2.2	0.5	1.7	1.2	0.7	1.4
T1	min	1125.7	13481.8	6.3	536.9	33044.0	0.2	0.1	0.9	13.3	0.3	0.4

	max	3312.9	42197.2	914.7	1470.6	88033.8	4.5	1.8	121.8	1178.5	3.5	22.0
	mean	2078.3	19230.5	139.8	985.9	48369.3	0.8	0.5	19.1	190.2	1.1	5.1
	SD	600.5	8846.6	293.5	302.7	16108.6	1.4	0.5	38.9	374.8	1.0	6.6
	CV	0.3	0.5	2.1	0.3	0.3	1.8	1.0	2.0	2.0	0.9	1.3
	VC	1.3	0.1	0.0	0.8	0.3	0.0	0.3	0.0	0.0	0.2	0.2
TT2	min	321.0	12048.8	4.7	272.8	23873.4	0.1	0.2	0.8	10.4	0.3	0.7
	max	2524.5	20756.5	568.0	1017.1	39335.1	2.0	1.3	57.1	1116.2	2.7	22.2
	mean	1148.1	16898.0	97.0	551.6	32228.7	0.4	0.4	10.2	173.2	0.9	8.0
	SD	727.9	2945.5	179.7	244.1	4615.5	0.6	0.4	17.9	357.5	0.7	7.7
	CV	0.6	0.2	1.9	0.4	0.1	1.5	0.9	1.8	2.1	0.8	1.0
	VC	0.9	0.8	0.1	0.6	0.5	0.1	0.3	0.1	0.1	0.3	0.2

1

2

1 Table 5. Statistics of element concentration (in $\mu\text{g l}^{-1}$) from selected stream, tributary and active rock glacier springs in the Sulden catchment
 2 sampled from March to October 2015. CV: coefficient of variation. VC: variability coefficient (see Eq. 1) with $\text{SD}_{\text{baseflow}}$ (based on samples
 3 from March, April, and October 2015) and $\text{SD}_{\text{melting}}$ (based on samples from May to September 2015). Note that CV was not calculated for
 4 SSPR2 – 4 as water samples were available only during summer.

location	statistics	Zn	As	Se	Rb	Sr	Ag	Cd	Sb	Hg	Pb	U
S1	min	4.1	12.1	0.5	0.0	307.9	0.0	0.0	0.2	0.0	0.4	0.0
	max	23.2	61.1	1.1	2.6	390.5	0.1	0.1	0.5	0.2	7.6	11.3
	mean	9.7	27.0	0.8	1.1	349.8	0.0	0.1	0.3	0.1	2.1	5.1
	SD	5.8	15.5	0.2	1.1	27.2	0.0	0.1	0.1	0.1	2.3	5.2
	CV	0.6	0.6	0.2	1.0	0.1	2.6	1.0	0.4	1.1	1.1	1.0
	VC	0.2	2.6	1.0	0.0	0.7	-	1.0	2.0	0.0	0.1	0.0
S2	min	3.7	15.1	0.4	0.0	334.0	0.0	0.0	0.1	0.0	0.3	0.0
	max	23.8	40.9	0.7	3.4	609.9	0.0	0.1	0.2	0.2	9.4	11.3
	mean	8.5	23.3	0.5	1.6	410.7	0.0	0.0	0.2	0.1	2.7	4.9
	SD	6.4	8.0	0.1	1.6	81.0	0.0	0.0	0.0	0.1	3.4	5.1

	CV	0.7	0.3	0.2	1.0	0.2	-	1.3	0.3	1.1	1.3	1.0
	VC	0.2	2.0	0.5	0.0	0.3	-	1.0	1.0	0.0	0.1	0.0
S6	min	5.6	6.3	0.5	0.0	524.0	0.0	0.0	0.3	0.0	0.4	0.0
	max	40.9	17.0	1.2	1.9	2024.0	0.0	0.2	0.5	0.1	18.1	11.3
	mean	19.1	10.1	0.9	0.7	1380.5	0.0	0.1	0.3	0.0	6.7	4.0
	SD	12.9	4.0	0.2	0.8	463.1	0.0	0.1	0.1	0.0	7.3	4.9
	CV	0.7	0.4	0.2	1.2	0.3	-	0.9	0.2	1.2	1.1	1.2
	VC	0.2	0.1	0.5	0.0	0.5	-	0.5	2.2	0.0	0.0	0.0
SSPR2-4	min	1.5	6.3	0.4	0.0	341.2	0.0	0.0	0.1	0.0	0.2	0.0
	max	49.4	38.0	0.6	2.7	1355.7	0.1	0.4	0.4	0.1	19.8	27.2
	mean	10.7	31.1	0.5	0.9	770.9	0.0	0.1	0.2	0.0	3.1	6.9
	SD	14.8	4.4	0.1	1.0	435.7	0.0	0.1	0.1	0.0	6.3	9.4
	CV	1.4	0.1	0.2	1.1	0.6	2.6	1.4	0.6	1.3	2.0	1.4

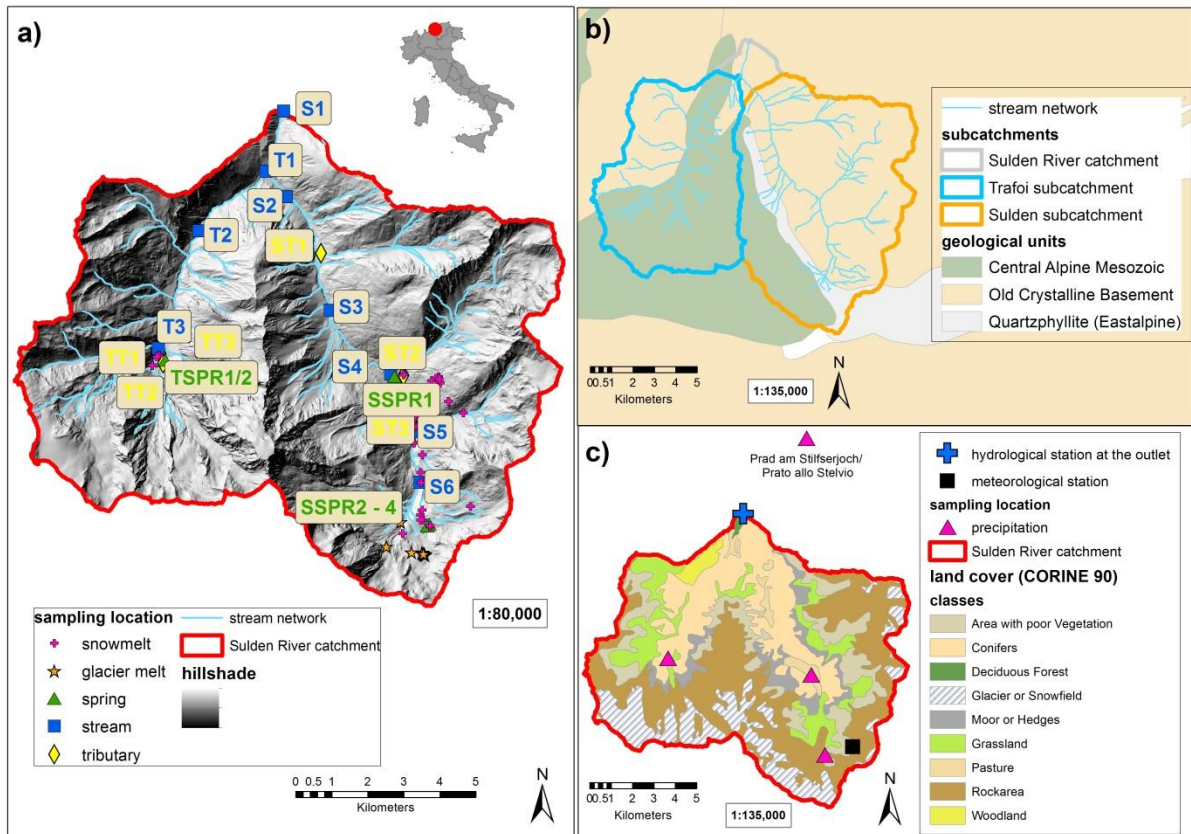
T1	min	2.3	7.2	0.6	0.0	220.9	0.0	0.0	0.2	0.0	0.3	0.0
	max	46.5	64.2	1.4	1.9	478.1	0.0	0.2	0.7	0.2	18.0	12.5
	mean	10.9	24.5	1.1	0.7	340.1	0.0	0.1	0.4	0.1	2.9	5.6
	SD	13.6	18.4	0.3	0.7	75.8	0.0	0.1	0.1	0.1	5.7	5.7
	CV	1.2	0.8	0.2	1.1	0.2	-	1.4	0.4	1.1	2.0	1.0
	VC	0.1	2.9	0.6	0.0	0.9	-	0.6	2.0	0.0	0.0	0.0
TT2	min	2.8	0.3	0.5	0.0	149.4	0.0	0.0	0.2	0.0	0.3	0.0
	max	39.4	1.2	1.5	1.7	384.5	0.5	0.1	0.5	0.7	9.1	10.6
	mean	9.9	0.7	1.0	0.4	247.5	0.1	0.0	0.3	0.1	1.8	4.8
	SD	11.4	0.3	0.3	0.5	67.5	0.2	0.0	0.1	0.2	2.8	4.9
	CV	1.2	0.4	0.3	1.5	0.3	2.6	1.3	0.4	1.8	1.5	1.0
	VC	0.1	0.3	1.3	0.0	1.2	0.0	1.0	-	0.0	0.1	0.0

1 Table 6. Variability coefficient (VC) for selected locations along the Sulden and Trafoi River
2 in 2014 and 2015.

Location	River section	VC
	(in km)	
T3	6.529	0.70
T2	2.774	0.85
T1	51	1.09
S6	12.87	0.01
S3	6.417	0.42
S2	2.739	0.35
S1	0	0.77

3

4

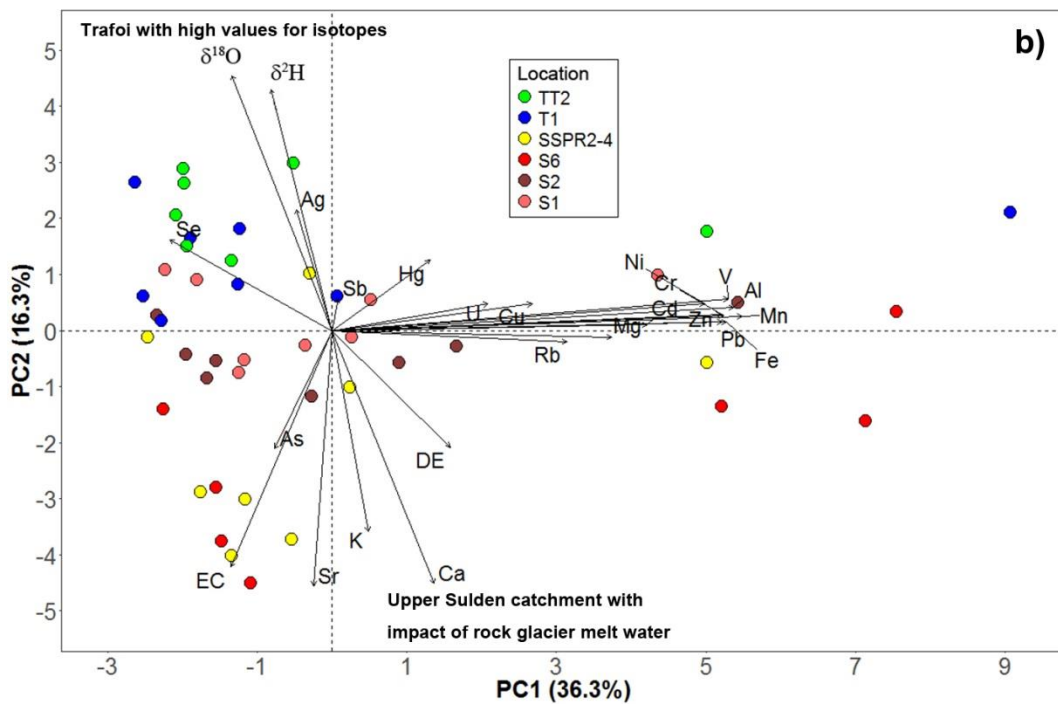
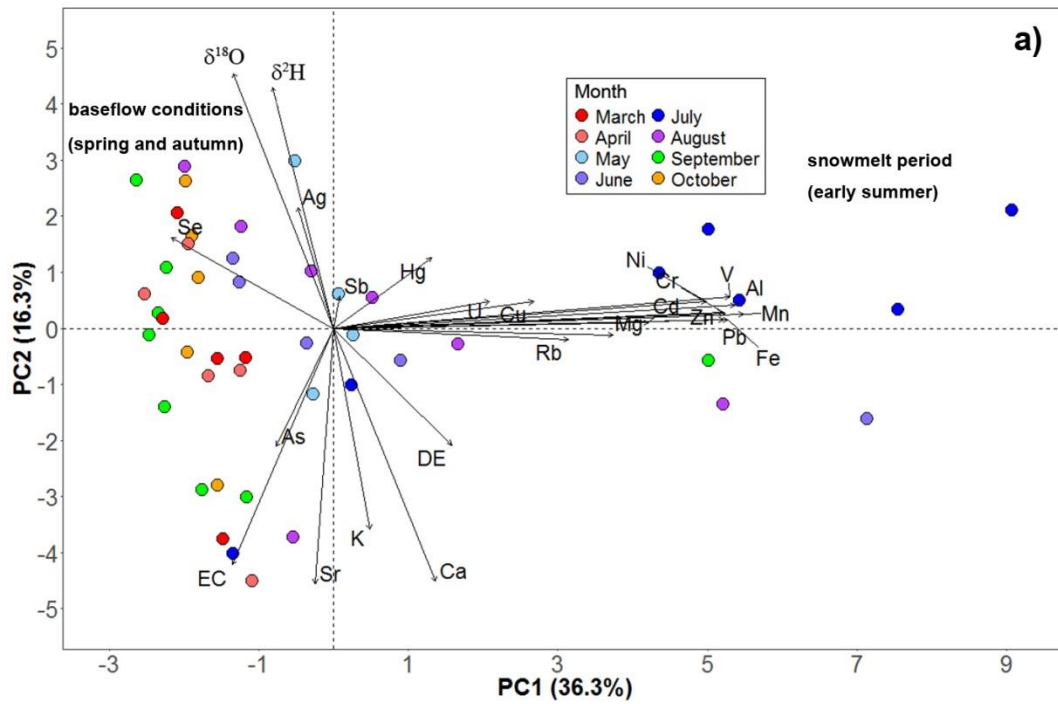


1

2 **Figure 1. Overview of the Sulden catchment with a) sampling point, b) geology, and c) land cover with**
 3 **instrumentation. The meteorological station shown is the Madritsch/Madriccio AWS of the Hydrographic Office**
 4 **(Autonomous Province of Bozen-Bolzano). The glacier extent refers to 2006 (Autonomous Province of Bozen-**
 5 **Bolzano).**

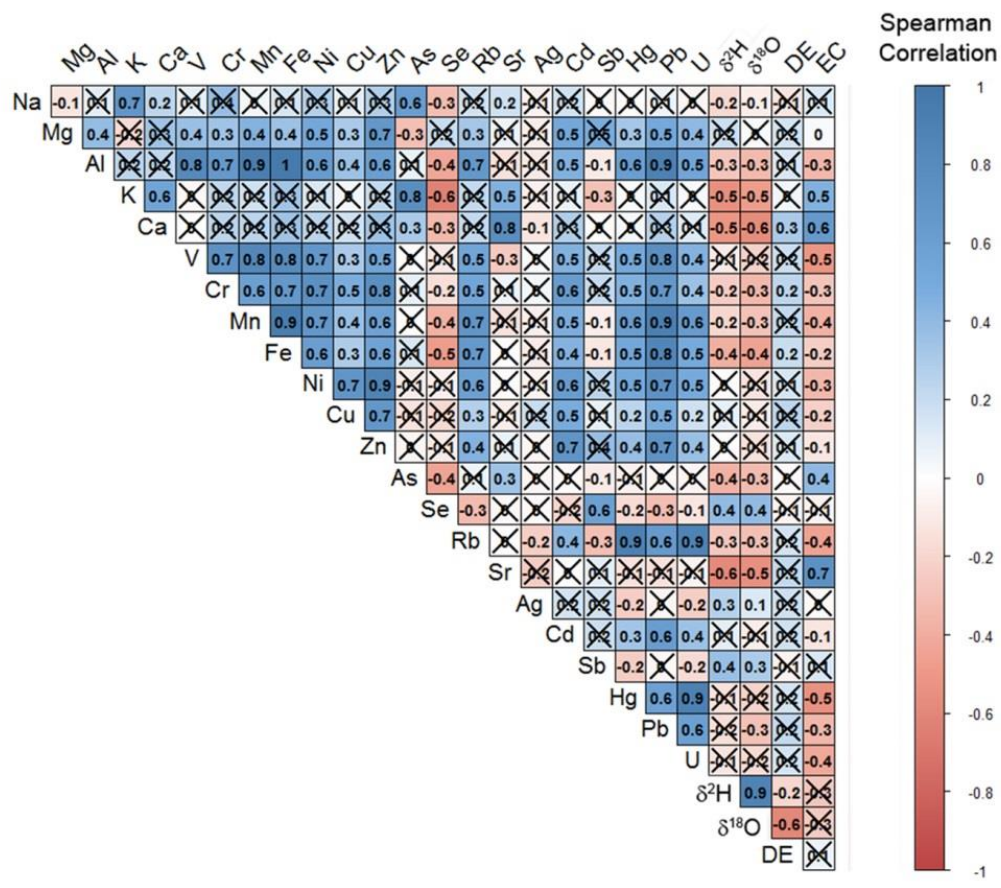
6

7



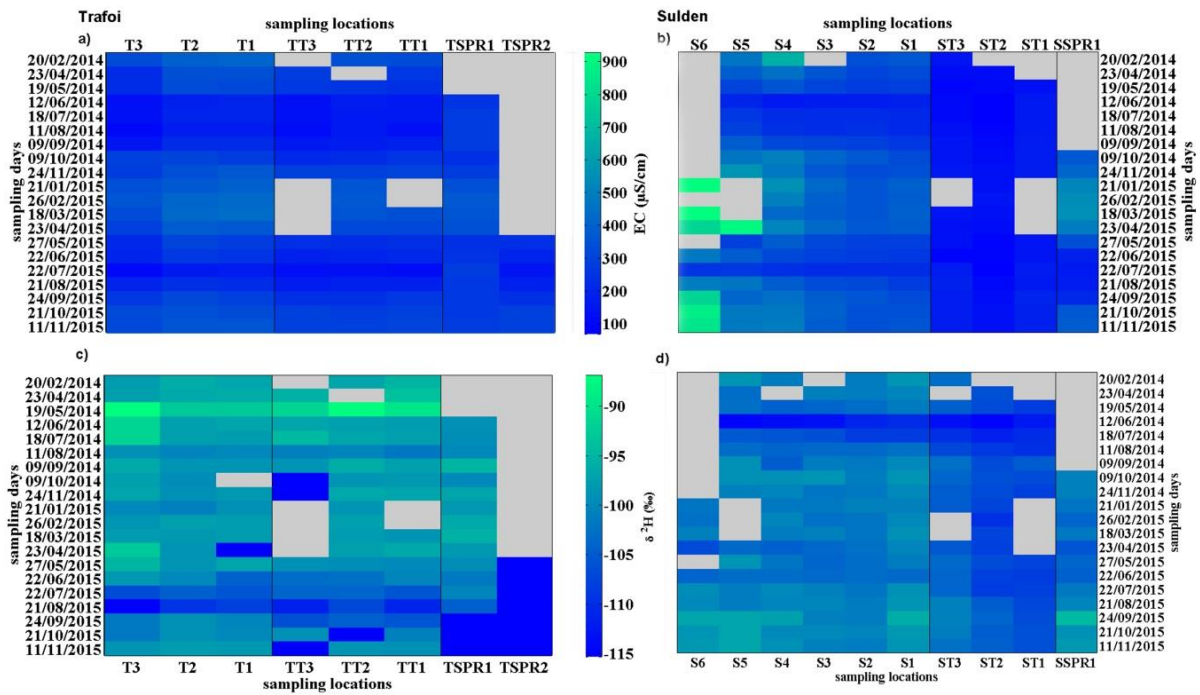
1
2
3
4
5
6

Figure 2. Principle component analysis of element concentrations of stream water and springs draining a rock glacier sampled in the Suldén and Trafoi sub-catchments from March to October 2015. Data based on n = 47 samples are shown in groups according to a) the sampling locations and b) the sampling month.



- 1
- 2
- 3
- 4
- 5

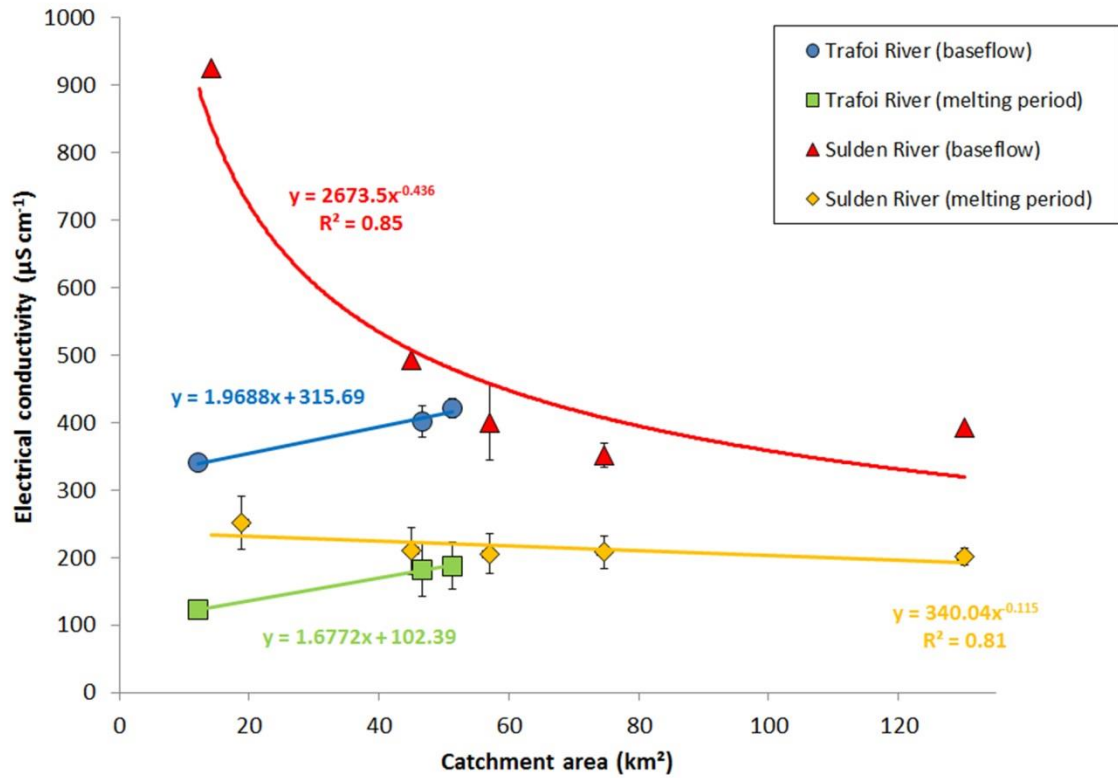
Figure 3. Spearman rank correlation matrix of hydrochemical variables. Values are shown for a level of significance $p < 0.05$, otherwise crossed out.



1
2
3
4
5
6
7

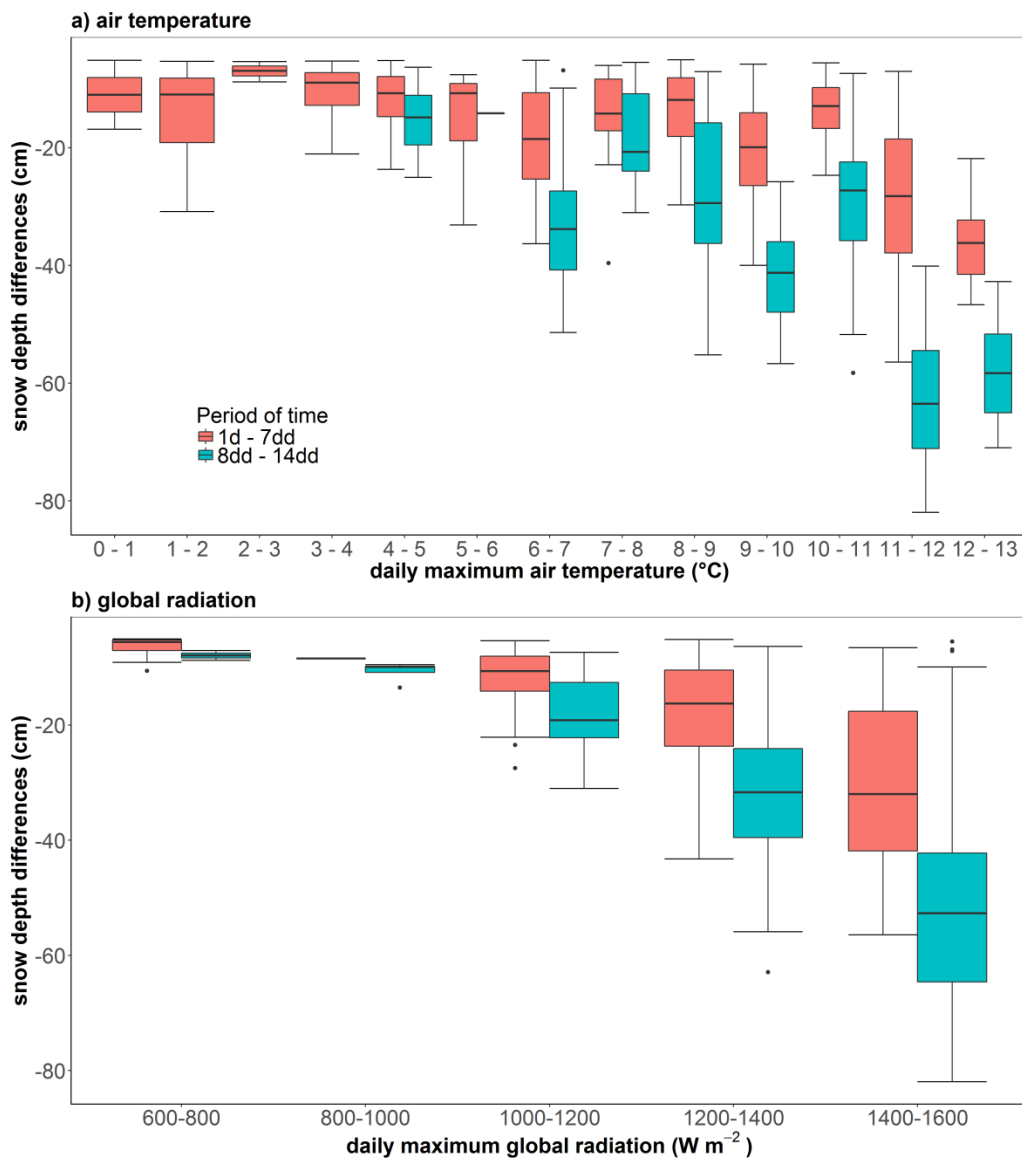
Figure 4. Spatial and temporal variability of EC ($\mu\text{S cm}^{-1}$) and $\delta^2\text{H}$ (‰) at different stream sections, tributaries and springs within the Trafoi sub-catchment (subplot a and c) and the Suldén sub-catchment (subplot b and d) in 2014 and 2015. The heatmaps are grouped into locations at streams, tributaries, and springs. Grey areas refer to missing sample values due to frozen or dried out streams/tributaries or because the sampling location was included later in the sampling scheme.

1

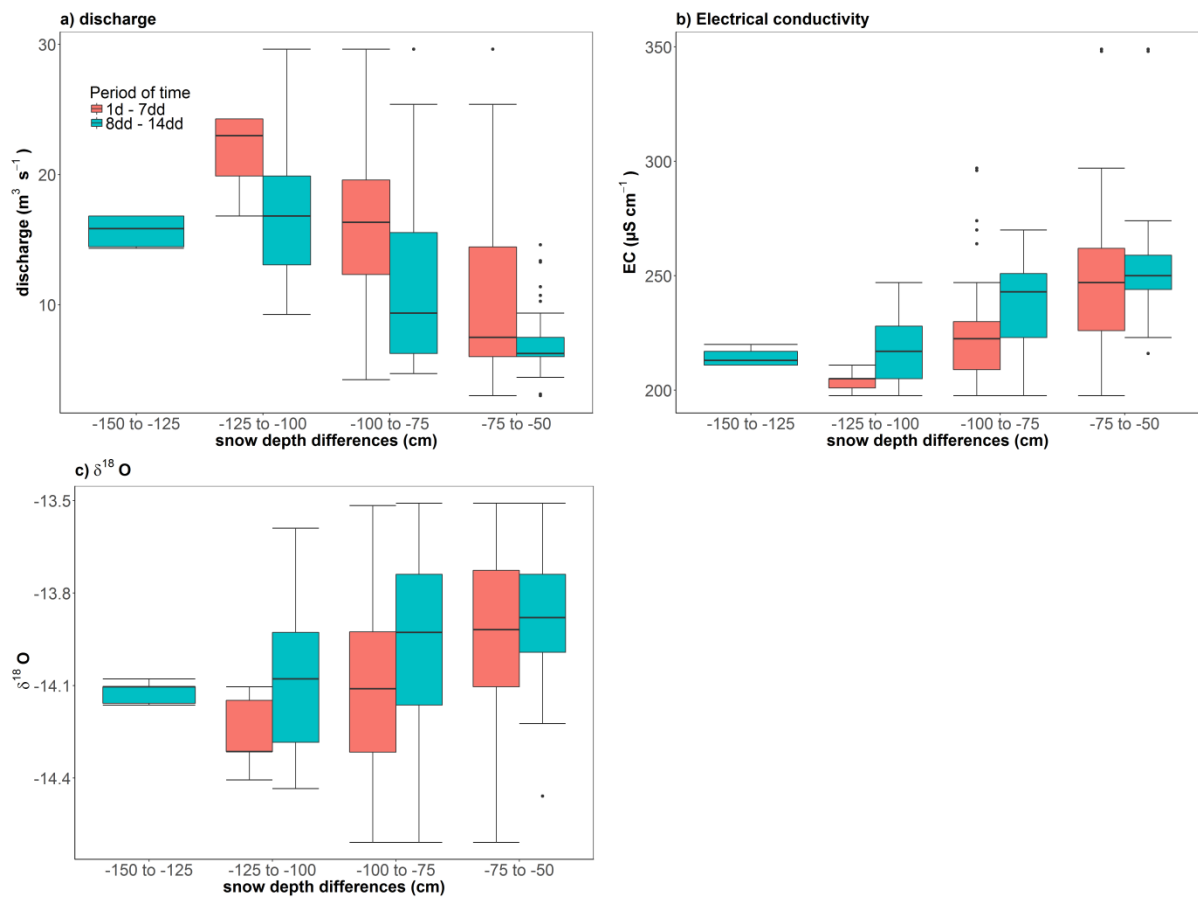


2

3 Figure 5. Spatial variability of electrical conductivity along the Trafoi and Sulden River against catchment area.
4 Electrical conductivity is averaged for sampling days during baseflow conditions (21/01/2015, 26/02/2015, and
5 18/03/2015) and melt period (12/06/2014, 18/07/2014, 11/08/2014, and 09/09/2014).



1
 2 **Figure 6. Box-plots of environmental variables a) daily maximum air temperature and b) daily maximum global**
 3 **radiation on snowmelt expressed as snow depth differences at AWS Madritsch. Snow depth differences smaller than**
 4 **5 cm are discarded from analysis.**

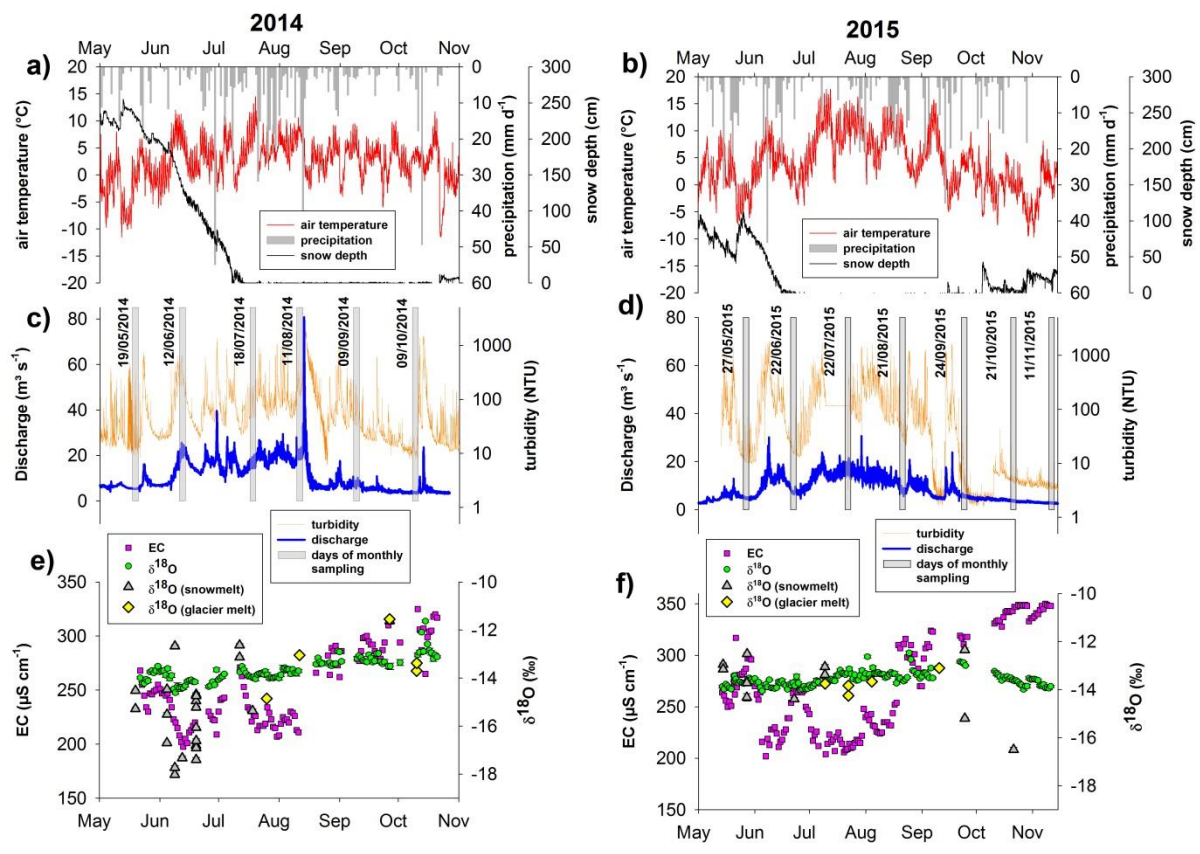


1

2 **Figure 7. Box-plots of snowmelt expressed as snow depth differences at AWS Madritsch on the variability of a)**
 3 **discharge, b) EC, and c) $\delta^{18}\text{O}$ at the outlet Stilfserbrücke in 2014 and 2015.**

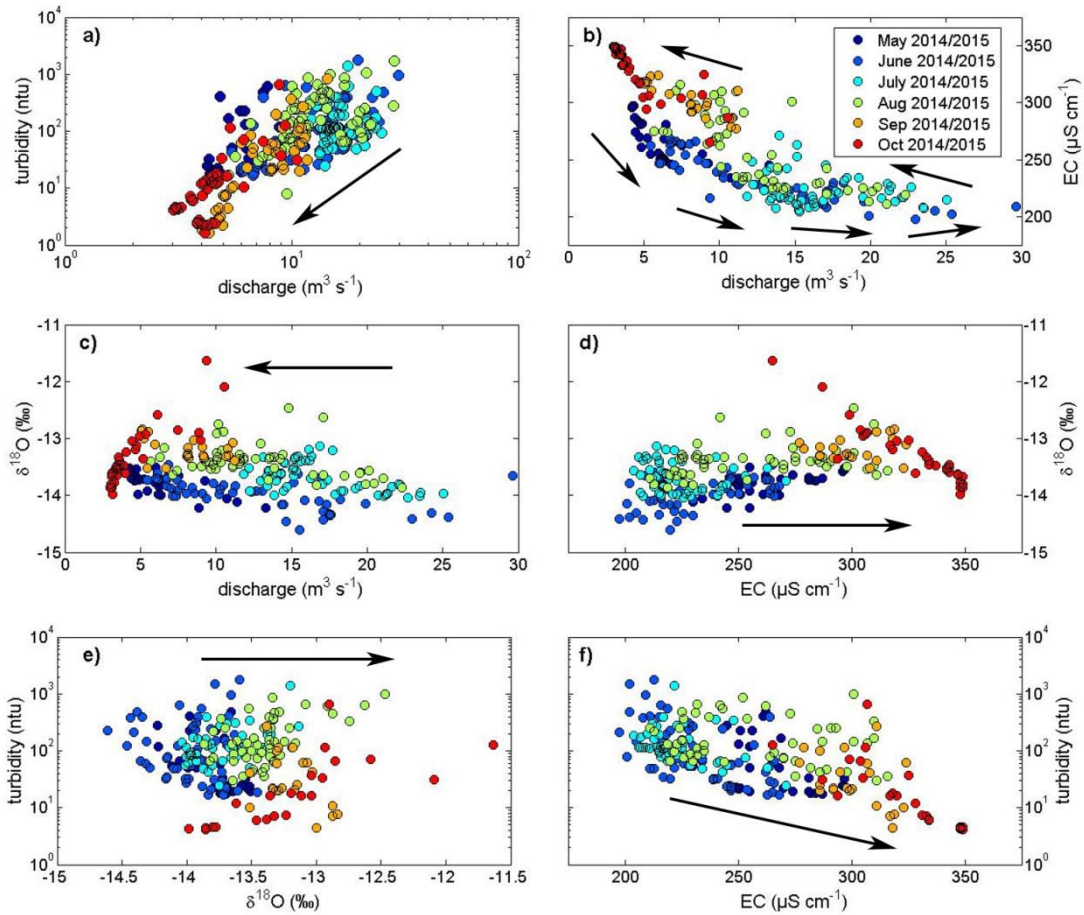
4

5

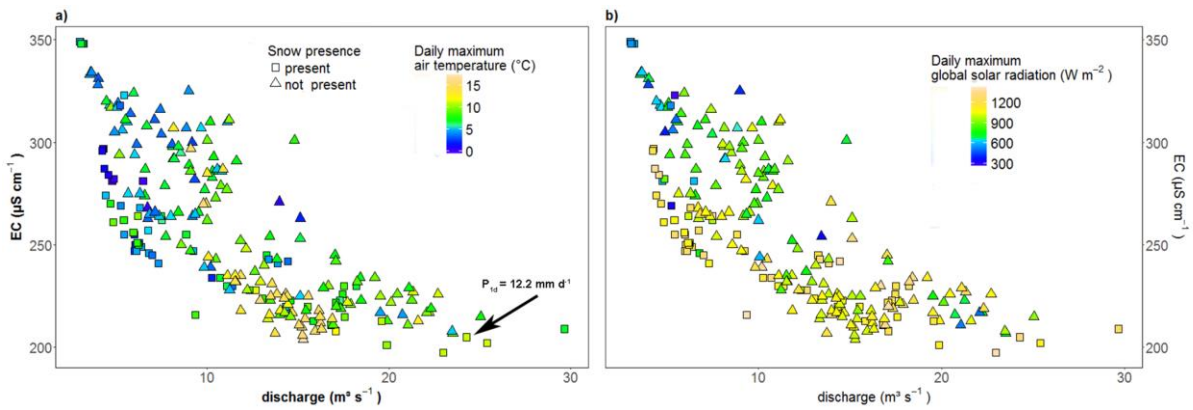


1
2
3
4
5
6

Figure 8. Time series from 2014 and 2015 of a) and b) precipitation, hourly air temperature and snow depth at the AWS Madritsch, c) and d) streamflow and turbidity, e) and f) electrical conductivity and $\delta^{18}\text{O}$ of the stream at the outlet Stilsferbrücke and of snowmelt and glacier melt water. Grey shaded bars indicate the date of monthly sampling carried out in the entire catchment.



1
 2 **Figure 9.** Monthly relationships between a) to e) discharge, turbidity and tracers such as EC and $\delta^{18}\text{O}$ at the outlet
 3 **Stilsferbrücke** in 2014 and 2015. The dataset consists of $n = 309$ samples. Arrows underline the monthly pattern.



4
 5 **Figure 10.** Monthly relationships between discharge and electrical conductivity (EC) at the outlet **Stilsferbrücke** with
 6 respect to a) daily maximum air temperature (1d) and b) daily maximum global solar radiation (1d) compared to the
 7 snow presence measured at the AWS **Madritsch** in 2014 and 2015.